

SAMPLING FOR APPROXIMATING R -LIMITED FUNCTIONS

CAN EVREN YARMAN

ABSTRACT. R -limited functions are multivariate generalization of band-limited functions whose Fourier transforms are supported within a compact region $R \subset \mathbb{R}^n$. In this work, we generalize sampling and interpolation theorems for band-limited functions to R -limited functions. More precisely, we investigated the following question: “For a function compactly supported within a region similar to R , does there exist an R -limited function that agrees with the function over its support for a desired accuracy?”. Starting with the Fourier domain definition of an R -limited function, we write the equivalent convolution and a discrete Fourier transform representations for R -limited functions through approximation of the convolution kernel using a discrete subset of Fourier basis. The accuracy of the approximation of the convolution kernel determines the accuracy of the discrete Fourier representation. Construction of the discretization can be achieved using the tools from approximation theory as demonstrated in the appendices. The main contribution of this work is proving the equivalence between the discretization of the Fourier and convolution representations of R -limited functions. Here discrete convolution representation is restricted to shifts over a compactly supported region similar to R . We show that discrete shifts for the convolution representation are equivalent to the spectral parameters used in discretization of the Fourier representation of the convolution kernel. This result is a generalization of the cardinal theorem of interpolation of band-limited functions. The error corresponding to discrete convolution representation is also bounded by the approximation of the convolution kernel using discretized Fourier basis.

1. INTRODUCTION

R -limited functions are functions whose Fourier transforms are supported within a region $R \subset \mathbb{R}^n$. They are multivariate generalization of band-limited functions. The terminology was coined by Slepian in [22]. In this work, we generalize sampling and interpolation theorems for band-limited functions to R -limited functions. Specifically, we explore answers to the following questions: “For a function compactly supported within a region similar to R , does there exist an R -limited function that agrees with the function over its support? If so, how shall we sample the function to construct an R -limited function that approximates the original function within a desired accuracy?”. The first question has been answered in [22]. Combining these results with methods from approximation theory, we answer the second question. Answering how to sample also provides a guide for where to sample.

In our exposition we choose an approximation theory perspective which provides an alternative insight to understanding of band-limited functions through discretization of the sine cardinal function as well as a deterministic framework for constructing sampling schemes for R -limited functions. Starting with the Fourier domain definition of a R -limited function, we write the equivalent convolution representation and write a discrete Fourier transform representation for R -limited functions

through approximation of the convolution kernel using a discrete subset of Fourier basis. The accuracy of the approximation of the kernel determines the accuracy of the discrete Fourier representation. Construction of the discretization can be achieved using the tools from approximation theory such as generalization of Padé approximation, which is summarized in Appendix A.

Our main results, Theorems 10 and 12, prove the equivalence between the discretization of the Fourier and convolution representations that approximate a compactly supported function within a region similar to R . We show that discrete shifts for the convolution representation are equivalent to the spectral parameters used in discretization of the Fourier representation of the convolution kernel. Discretization of the convolution representation is also referred to as sampling and interpolation theorem.

Theorem 12 is a generalization of the sampling and interpolation theorem for band-limited functions summarized in Theorem 7. It also provides a way to analyze and approximate the resulting error. We show that the error corresponding to discrete convolution representation is bounded by error obtained from discretization of the Fourier transform of the convolution kernel. In single dimension, it provides a new way to prove truncation of discrete Fourier series as well as sinc interpolation formula. Furthermore, in single dimension, our result indicates that for a support of interest, instead of uniform sampling, improvement in discrete the Fourier representation of band-limited functions can be obtained using Gauss-Legendre type quadratures (see Appendix A). This also raises the questions on what is the most cost efficient way to implement fast Fourier transforms using Gaussian quadratures which may be addressed using the ideas from [6, 5, 7, 12] and left for a future discussion. Similar discretizations are obtained for special cases of R -limited functions in Appendix C and D where we make use of cascaded quadratures that are equivalent to Gauss-Legendre or Clenshaw-Curtis quadratures. While the body of the manuscript contains our main results, the Appendices also provide as valuable information by providing a constructive way for computing quadratures to discretize convolution kernels which can be utilized in the sampling and interpolation theorems.

The outline of the manuscript is as follows. In Section 2, we present the conventions used in the rest of our discussion. To motivate the multivariate case, in Section 3, we study discretization of Fourier transform and sinc interpolation formula for one-dimensional (univariate) band-limited functions, or band-limited projection of compactly supported functions. Both discrete Fourier transform and sinc interpolation formulas have been studied in the literature with many books devoted to this topic. We refer the reader to [13, 27, 26, 14] for a comprehensive list of references on these topics. We give an alternative exposition, which leads to proof of the equivalence of sampling in the domain of the function (Theorem 7) and its Fourier transform (Theorem 1). The necessary background material for Section 3 is provided in Appendices A and B which discuss Generalization of Pade approximation and approximations to sine cardinal function. Compared to band-limited function, sampling and representation of multivariate functions whose Fourier transforms' support are not similar to a hypercube is studied and understood less. In Section 4, we extend our results for band-limited function (Theorems 1 and 7) to R -limited functions (Theorems 10 and 12). Examples of special cases of convolution kernels for R -limited functions are presented in Appendices C and

D. In Appendix C, we provide a method to construct quadratures for isosceles triangle and trirectangular tetrahedron which are used to construct quadratures for equilateral triangle and regular tetrahedron. Similar method is used in Appendix D to construct quadratures for a finite cone and a ball in three dimensions which have practical importance in multidimensional signal processing seismic data, image processing and video processing.

2. CONVENTIONS

We employ the following conventions of Fourier transform, inverse Fourier transform and convolution.

The *Fourier transform* $\mathcal{F}[f](\mathbf{k})$ of $f(\mathbf{x})$, an absolutely integrable function for $\mathbf{x}, \mathbf{k} \in \mathbb{R}^N$, which we denote by $\hat{f}(\mathbf{k})$, is defined by

$$(2.1) \quad \mathcal{F}[f](\mathbf{k}) = \hat{f}(\mathbf{k}) = \int_{\mathbb{R}^N} f(\mathbf{x}) e^{-i2\pi\mathbf{k}\cdot\mathbf{x}} d\mathbf{x}$$

The *inverse Fourier transform* is defined by

$$(2.2) \quad \mathcal{F}^{-1}[\hat{f}](\mathbf{x}) = f(\mathbf{x}) = \int_{\mathbb{R}^N} \hat{f}(\mathbf{k}) e^{i2\pi\mathbf{k}\cdot\mathbf{x}} d\mathbf{k}$$

Denoting the *convolution* operator by $*$, convolution of two functions is defined by

$$(2.3) \quad (f * g)(\mathbf{x}) = \int_{\mathbb{R}^N} f(\mathbf{y}) g(\mathbf{x} - \mathbf{y}) d\mathbf{y}$$

The Fourier transform of the convolutions is the product of the Fourier transforms:

$$(2.4) \quad \mathcal{F}[f * g](\mathbf{k}) = \hat{f}(\mathbf{k}) \hat{g}(\mathbf{k})$$

also referred to as convolution theorem.

3. BAND-LIMITED FUNCTIONS

We say that $f_B(t)$, for $t \in \mathbb{R}$, is a *band-limited* function with band-limit B if there exists an $\hat{f}_B(\omega)$ such that

$$(3.1) \quad \begin{aligned} f_B(t) &= \int_{-B}^B \hat{f}_B(\omega) e^{i2\pi t\omega} d\omega \\ &= B \int_{-1}^1 \hat{f}_B(B\omega) e^{i2\pi Bt\omega} d\omega \end{aligned}$$

Given a function $f(t)$, its *band-limited projection* $P_B[f](t)$, denoted by $f_B(t)$ for short, is defined by

$$(3.2) \quad \begin{aligned} P_B[f](t) = f_B(t) &= \int_{-B}^B \hat{f}(\omega) e^{i2\pi t\omega} d\omega \\ &= B \int_{-1}^1 \hat{f}(B\omega) e^{i2\pi Bt\omega} d\omega \end{aligned}$$

or, equivalently, in the convolution representation using Parseval's theorem

$$(3.3) \quad P_B[f](t) = f_B(t) = \int_{-\infty}^{\infty} f(\tau) 2B \operatorname{sinc}(2\pi B[t - \tau]) d\tau$$

where

$$(3.4) \quad \text{sinc}(Bt) = \frac{1}{2B} \int_{-B}^B e^{i\omega t} d\omega = \int_0^1 \cos(B\omega t) d\omega = \frac{\sin(Bt)}{Bt}$$

is the sinc function normalized with band-limit B . Note that

$$(3.5) \quad \hat{f}_B(\omega) = \hat{f}(\omega), \quad \omega \in [-B, B]$$

3.1. Discrete Fourier representation of band-limited approximation of compactly supported functions: In this section we derive discrete Fourier approximations of band-limited projection of compactly supported functions starting from their convolution representation.

Consider a discretization of the integral representation of sinc (see Figures B.1 and B.3 for two examples. Another example in Section 8 of [1].)

$$(3.6) \quad \begin{aligned} 2B \text{sinc}(Bt) &= 2 \int_0^B \cos(\omega t) d\omega \\ &= \sum_{m=1}^M 2\alpha_m \cos(B\omega_m t) + \alpha_0 + \epsilon_B(t) \end{aligned}$$

for a given $B \in \mathbb{R}^+$, with $\alpha_m \in \mathbb{R}^+$ and $\omega_m \in [0, 1]$. Equivalently, using exponentials instead of cosines, we write

$$(3.7) \quad 2B \text{sinc}(Bt) = \int_{-B}^B e^{i\omega t} d\omega = \sum_{m=-M}^M \alpha_m e^{iB\omega_m t} + \epsilon_B(t)$$

where $-\omega_m = \omega_{-m}$ and $\alpha_{-m} = \alpha_m$. Now we can prove:

Theorem 1. *Given a compactly supported function $f(t)$ over $[-T, T]$, restriction of its band-limited projection, $f_B(t)$, onto interval $[-T, T]$ can be approximated as a discrete sum of Fourier basis by*

$$(3.8) \quad f_B(t) = \sum_{m=-M}^M \alpha_m \hat{f}(B\omega_m) e^{i2\pi B\omega_m t} + \epsilon_f(t)$$

using the approximation (3.7) with the error bound

$$(3.9) \quad \max_{t \in [-T, T]} |\epsilon_f(t)| \leq 2T \max_{t \in [-T, T]} |f(t)| \max_{t \in [-2T, 2T]} |\epsilon_B(2\pi t)|.$$

Proof. For a function $f(\tau)$ compactly supported on $\tau \in [-T, T]$, substituting (3.7) into (3.3), its band-limited projection can be approximated by (3.8) where

$$(3.10) \quad \epsilon_f(t) = \int_{-T}^T f(\tau) \epsilon_B(2\pi[t - \tau]) d\tau$$

(3.8) provides a discretization of (3.2) through approximation of the sinc function as a sum of cosines. \square

Example 2. Choosing

$$(3.11) \quad (\alpha_m, \omega_m)_{m=-M}^M = \left(\frac{2B}{2M+1}, \frac{2m}{2M+1} \right)_{m=-M}^M$$

for some $M \geq 0$, (3.8) becomes the discrete Fourier transform representation of $f_B(t)$:

$$(3.12) \quad f_B(t) = \frac{2B}{2M+1} \sum_{m=-M}^M \hat{f}\left(B \frac{2m}{M+1}\right) e^{i2\pi B \frac{2m}{2M+1} t} + \epsilon_f(t)$$

The summation term is referred to as the *discrete inverse Fourier transform* of \hat{f} . (3.12) is a Riemann sum approximation of the integral (3.1) for uniform sampling of the interval $[-B, B]$.

In practice measurements are performed over a finite duration. Thus it is desirable to have the band-limited projection of a compactly supported function approximately agree with the function at least over $t \in [-T, T]$. Thus, by (3.9), for $f_B(t)$ to approximate accurately $f(t)$ over $[-T, T]$, one needs to build up an approximation to $\text{sinc}(Bt)$ that is accurate over the interval $[-4\pi T, 4\pi T]$. In Appendix B, we present two different approximations in the form of (3.7) (see Figures B.1 and B.3), one using Gauss-Legendre quadratures (see Figure B.2) and the other using uniform sampling. We show that, for a desired interval and bandwidth, a discrete representation of sinc that is accurate upto machine precision can be achieved using Gauss-Legendre quadratures without requiring as many uniform samples.

Example 3. From a finite duration measurement, only finite number of samples are utilized for digital signal processing. This raises a natural question: ‘‘What should be the sampling rate for a band-limited measurement such that band-limited projection of the the discrete measurement agree with with the discrete measurement?’’. In this regard, consider the following model for a discrete measurement

$$(3.13) \quad f(t) = \sum_{k=-K}^K f_k \delta\left(t - \frac{2k}{2K+1} T\right)$$

where $2T/(2K+1)$ is the sampling period. Then

$$(3.14) \quad \hat{f}(\omega) = \sum_{k=-K}^K f_k e^{-i2\pi\omega \frac{2k}{2K+1} T}$$

Assuming that the measurement has band-limit B , let $\omega_m = B 2m (2M+1)^{-1}$. By (3.14), we rewrite (3.12) in terms of $\hat{f}(\omega_m)$ and obtain

$$(3.15) \quad f_B(t) = \frac{2B}{2M+1} \sum_{k=-K}^K f_k \left(\sum_{m=-M}^M e^{i2\pi B \frac{2m}{2M+1} (t - \frac{2k}{2K+1} T)} \right) + \epsilon_f(t)$$

which, for $t = 2l/(2K+1)T$, $l = -K, \dots, K$, becomes

$$(3.16) \quad f_B\left(\frac{2l}{2K+1}T\right) = \frac{2B}{2M+1} \sum_{k=-K}^K f_k \left(\sum_{m=-M}^M e^{i2\pi B \frac{2m}{2M+1} \frac{2T}{2K+1} (l-k)} \right) + \epsilon_f\left(\frac{2l}{2K+1}T\right)$$

(3.14) is known as the *discrete Fourier transform* of the vector $\{f_k\}_{k=-K}^K$.

For $T = (2K + 1)/(4B)$, (3.13), (3.14) for $\omega = B 2m(2M + 1)^{-1}$, and (3.16) become

$$(3.17) \quad f(t) = \sum_{k=-K}^K f_k \delta\left(t - \frac{k}{2B}\right)$$

$$(3.18) \quad \hat{f}\left(B \frac{2m}{2M+1}\right) = \sum_{k=-K}^K f_k e^{-i2\pi \frac{m}{2M+1} k}$$

$$(3.19) \quad f_B\left(\frac{l}{2B}\right) = \frac{2B}{2M+1} \sum_{k=-K}^K f_k \left(\sum_{m=-M}^M e^{i2\pi \frac{m}{2M+1} (l-k)} \right) + \epsilon_f\left(\frac{l}{2B}\right)$$

which, for $|l - k| \leq 2M$, is

$$(3.20) \quad f_B\left(\frac{l}{2B}\right) = 2B \sum_{k=-K}^K f_k \delta_{kl} + \epsilon_f\left(\frac{l}{2B}\right) = 2B f_l + \epsilon_f\left(\frac{l}{2B}\right),$$

where δ_{kl} is the Kronecker delta function.¹ The inequality $|l - k| \leq 2M$ imposes that $M \geq K$. For $T = (2K + 1)/(4B)$, by (3.13) and (3.7), (3.10) becomes

$$(3.21) \quad \begin{aligned} \epsilon_f\left(\frac{l}{2B}\right) &= \int_{-T}^T f(\tau) \epsilon_B\left(2\pi \left[t - \frac{l}{2B}\right]\right) d\tau \\ &= \sum_{k=-K}^K f_k \epsilon_B\left(2\pi \left[\frac{k}{2B} - \frac{l}{2B}\right]\right) \\ &= \sum_{k=-K}^K f_k \left[\begin{array}{l} 2B \text{sinc}(\pi [k - l]) \\ - \left(\frac{2B}{2M+1} \sum_{m=-M}^M e^{i2\pi \frac{m}{2M+1} (l-k)}\right) \end{array} \right] \\ &= \sum_{k=-K}^K f_k \left[2B \delta_{k,l} - \frac{2B}{2M+1} (2M+1) \delta_{k,l} \right] \\ &= 0. \end{aligned}$$

The special sampling rate $1/(2B)$ that gave rise to the band-limited function $f_B(t)$ whose values are equal to the original function at $t = l/(2B)$. This sampling rate is referred to as the Nyquist rate. By sinc interpolation, also known as Whittaker-Shannon interpolation formula [26],

$$(3.22) \quad f_B(t) = \sum_{k=-\infty}^{\infty} f_B\left(\frac{k}{2B}\right) \text{sinc}\left(2\pi B \left[t - \frac{k}{2B}\right]\right),$$

¹Consider (3.13) for $t = lT(K + 1)^{-1}$:

$$f\left(l \frac{T}{K+1}\right) = \sum_{k=-K}^K f_k \frac{K+1}{T} \delta(l - k).$$

For $T = (K + 1)/(2B)$, $f\left(\frac{l}{2B}\right) = 2B \sum_{k=-K}^K f_k \delta(l - k)$. Thus the factor $2B$ in front of the sum in (3.20) is due to difference between continuous and discrete nature of Dirac delta, $\delta(|l - k|(2B)^{-1}) = 2B \delta(l - k)$, and Kronecker delta, δ_{lk} , functions.

a band-limited function can be exactly determined from samples obtained using Nyquist rate. In digital signal processing, because finitely many samples are measured, which are modelled by (3.17), (3.22) is approximated by

$$(3.23) \quad f_B(t) \approx \sum_{k=-K}^K f\left(\frac{k}{2B}\right) \operatorname{sinc}\left(2\pi B\left[t - \frac{k}{2B}\right]\right),$$

which is band-limited projection of (3.13). This approximation agrees with the discrete measurements. However, there is an approximation error between the sample locations as a result of implicit imposition $f(k(2B)^{-1})$ equal to zero for $|k| > K$. This imposition is eliminated when, instead of discrete Fourier basis, prolate spheroidal wave functions (PSWFs) are used as a basis to represent band-limited functions. Expressing band-limited function in terms of PSWFs doesn't directly answer how a band-limited function should be sampled but provides the necessary foundation to answer "How accurately can we approximate a band-limited function from its samples given over a compact support?", which is addressed in Theorem (7).

3.2. Band-limited projections of compactly supported function and prolate spheroidal wave functions. In this section we present prolate spheroidal wave functions, their properties and two methods on how we can numerically compute them. For the rest of our discussion we will assume that $T = 1$. This can be compensated by choosing the band-limit to be T times more.

3.2.1. *Prolate spheroidal wave functions (PSWF).* Prolate spheroidal wave functions (PSWF), $\varphi_n(t)$ can be defined as the eigenfunctions of the band-limited projection operator restricted to a compact support, which, without loss of generality, is given by [24, 20]

$$(3.24) \quad \int_{-1}^1 2B \operatorname{sinc}(2\pi B(t - \tau)) \varphi_n(\tau) d\tau = \mu_n \varphi_n(t), \quad t \in \mathbb{R}$$

PSWF form a basis for band-limited functions as well as $L_2([-1, 1])$, and satisfy the following properties [24, 20]:

- (1) PSWF are real valued and corresponding eigenvalues μ_n are positive: $\varphi_n(t) \in \mathbb{R}$, $\mu_n \in \mathbb{R}^+$.
- (2) PSWF are orthogonal within the interval $t \in [-1, 1]$ as well as over the real line:

$$(3.25) \quad \mu_n \int_{-\infty}^{\infty} \varphi_n(t) \varphi_m(t) dt = \int_{-1}^1 \varphi_n(t) \varphi_m(t) dt = \delta_{m,n}$$

where $\delta_{m,n}$ is the Kronocker delta function equal to 1 for $m = n$ and zero otherwise.

- (3) PSWF are eigenfunctions of Fourier operator restricted to the interval $[-1, 1]$:

$$(3.26) \quad \int_{-1}^1 \varphi_n(t) e^{i2\pi B\omega t} dt = \lambda_n \varphi_n(\omega), \quad \omega \in [-1, 1], \lambda_n \in \mathbb{C}$$

The second property implies that if a band-limited function is known within an interval then it is known

The eigenvalues satisfy the following properties:

- (1) Multiplying both sides of (3.26) with $e^{-i2\pi B\omega t}$, integrating with respect to ω and comparing the result with (3.24) one obtains $\mu_n = B|\lambda_n|^2$ (see 3.48 in [20])
- (2) [[17],Theorem 3.14 in [20]] Let $N(\alpha)$ denote the number of eigenvalues $\mu_n > \alpha$ for some $0 < \alpha < 1$. Then

$$(3.27) \quad N(\alpha) = 4B + \left(\frac{1}{\pi^2} \log \left(\frac{1-\alpha}{\alpha} \right) \right) \log(2\pi B) + O(\log(2\pi B))$$

Thus there are about $4B$ eigenvalues μ_n that are close to one, on the order of $\log(2\pi B)$ eigenvalues that decay rapidly, and the rest of them are very close to zero.

For a comprehensive review on PSWF, we refer the reader to [20].

Lemma 4. *Given a compactly supported function $f(t)$ on $t \in [-1, 1]$, it can be expressed in terms of PSWFs by*

$$(3.28) \quad f(t) = \sum_n f_{B,n} \varphi_n(t)$$

where

$$(3.29) \quad \begin{aligned} f_{B,n} &= \int_{-1}^1 f(t) \varphi_n(t) dt \\ &= \frac{1}{\mu_n} \int_{-1}^1 f_B(t) \varphi_n(t) dt \\ &= \int_{-\infty}^{\infty} f_B(t) \varphi_n(t) dt \end{aligned}$$

Proof. Because $2B \operatorname{sinc}(2\pi B(t - \tau))$ is band-limited, it can be expanded as a sum of PSWF,

$$(3.30) \quad 2B \operatorname{sinc}(2\pi B(t - \tau)) = \sum_n a_n(\tau) \varphi_n(t),$$

where

$$(3.31) \quad a_n(\tau) = \int_{-1}^1 2B \operatorname{sinc}(2\pi B(t - \tau)) \varphi_n(t) dt = \mu_n \varphi_n(\tau)$$

leading to the decomposition of sinc in terms of PSWF:

$$(3.32) \quad 2B \operatorname{sinc}(2\pi B(t - \tau)) = \sum_n \mu_n \varphi_n(\tau) \varphi_n(t)$$

Given a compactly supported function $f(t)$ on $t \in [-1, 1]$, it's band-limited projection $f_B(t)$ can be expanded in term of PSWF by substituting (3.32) in (3.3)

$$(3.33) \quad f_B(t) = \sum_n \mu_n f_{B,n} \varphi_n(t).$$

Then, by (3.25), the coefficients can be computed by either of the three ways in (3.29). \square

3.2.2. *Approximating PSWF as eigenvectors of $e^{-i2\pi B\omega_k\omega_m}$.* Substituting (3.7) into (3.24), and recalling $\mu_n = B|\lambda_n|^2$, by (3.26), we obtain

$$\begin{aligned} \varphi_n(t) &= \frac{1}{\mu_n} \int_{-1}^1 2B \operatorname{sinc}(2\pi B(t-\tau)) \varphi_n(\tau) d\tau \\ (3.34) \quad &= \frac{1}{B\lambda_n} \sum_{m=-M}^M \alpha_m e^{i2\pi B\omega_m t} \varphi_n(\omega_m) + \epsilon_{\varphi_n}(t) \end{aligned}$$

where

$$(3.35) \quad \epsilon_{\varphi_n}(t) = \frac{1}{\mu_n} \int_{-1}^1 \epsilon_B(2\pi[t-\tau]) \varphi_n(\tau) d\tau$$

with ²

$$(3.36) \quad \max_{t \in [-1,1]} |\epsilon_{\varphi_n}(t)| \leq \frac{1}{\mu_n} \max_{t \in [-2,2]} |\epsilon_B(2\pi t)|$$

In [1] (see equation (8.19) and (8.20) in [1]), (3.34) was used to build approximate PSWFs by first solving the eigensystem

$$(3.37) \quad \varphi_n(\omega_k) = \frac{1}{B\lambda_n} \sum_{m=-M}^M \alpha_m e^{i2\pi B\omega_m\omega_k} \varphi_n(\omega_m)$$

for the eigenvector $\varphi_n(\omega_k)$, followed by substituting $\varphi_n(\omega_k)$ back in (3.34):

$$(3.38) \quad \varphi_n(t) = \frac{1}{B\lambda_n} \sum_{m=-M}^M \alpha_m e^{i2\pi B\omega_m t} \varphi_n(\omega_m) + \epsilon_{\varphi_n}(t)$$

where $\epsilon_{\varphi_n}(\omega_k) = 0$, for $k = -M, \dots, M$.

Thus, the eigensystem (3.37) provides an approximation to PSWF over the interval $[-1, 1]$ bounded by (3.36). Because (3.37) is a system of $2M + 1$ equations, it has $2M + 1$ eigenvalues, which we will denote by $\mu_{n=0, \dots, 2M}$. By (3.27), in order to capture the dominant eigenvalues, i.e. eigenvalues around 1, one shall have $M \geq \lceil 2B - 1/2 \rceil$.

For sake of simplicity of the discussion, we will assume that $M \gg \lceil 2B - 1/2 \rceil$, $\mu_{2M} \ll 1$. Thus the corresponding $2M + 1$ approximate PSWFs provides a sufficiently accurately approximate band-limited functions over the interval $[-1, 1]$ and, by the same token, sinc function over $[-2, 2]$. Thus we treat, (3.32) is equivalent to its truncated version:

$$(3.39) \quad 2B \operatorname{sinc}(2\pi B(t-\tau)) \approx \sum_{n=-M}^M \mu_n \varphi_n(\tau) \varphi_n(t), t, \tau \in [-1, 1],$$

and similarly all the infinite sums over PSWFs as finite sums.

²By Hölder's inequality,

$$\begin{aligned} |\epsilon_{\varphi_n}(t)|^2 &\leq \frac{1}{\mu_n^2} \int_{-1}^1 |\epsilon_B(2\pi[t-\tau])|^2 |\varphi_n(\tau)|^2 d\tau \\ &\leq \frac{1}{\mu_n^2} \max_{\tau \in [t-1, t+1]} |\epsilon_B(2\pi\tau)|^2 \underbrace{\int_{-1}^1 |\varphi_n(\tau)|^2 d\tau}_{=1} \end{aligned}$$

Example 5. Consider (3.26) and the quadratures of discrete inverse Fourier transform (3.11) for $B = \frac{2M+1}{4}$

$$(3.40) \quad (\alpha_m, \omega_m)_{m=-M}^M = \left(\frac{1}{2}, \frac{2m}{2M+1} \right)_{m=-M}^M$$

for some positive integer M . Then (3.34) becomes

$$(3.41) \quad \varphi_n(t) = \frac{1}{\lambda_n} \frac{2}{2M+1} \sum_{m=-M}^M e^{i\pi m t} \varphi_n \left(\frac{2m}{2M+1} \right) + \epsilon_{\varphi_n}(t)$$

Consequently, the eigensystem for approximate PSWF is

$$(3.42) \quad \varphi_n \left(\frac{2k}{2M+1} \right) = \frac{1}{\lambda_n} \frac{2}{2M+1} \sum_{m=-M}^M e^{i2\pi \frac{mk}{2M+1}} \varphi_n \left(\frac{2m}{2M+1} \right)$$

for $k = -M, \dots, M$, which for $M \geq 2$ has four distinct eigenvalues, $\pm 2\sqrt{2M+1}$ and $\pm i2\sqrt{2M+1}$ with multiplicities (see page 32 of [2]).

3.2.3. *Approximating PSWF as eigenvectors of sinc* $(2\pi B(\omega_m - \omega_k))$. An alternative to the method presented in Section 3.2.2, PSWF can be approximated through discretization of (3.24).

Starting with (3.34) and using (3.26), we have

$$(3.43) \quad \varphi_n(\omega) = \frac{1}{\lambda_n} \int_{-1}^1 e^{-i2\pi B\omega t} \varphi_n(t) dt$$

$$(3.44) \quad = \frac{1}{B\mu_n} \sum_{m=-M}^M \alpha_m 2B \operatorname{sinc}(2\pi B(\omega_m - \omega)) \varphi_n(\omega_m) + \varepsilon_{\varphi_n}(\omega)$$

where

$$(3.45) \quad \varepsilon_{\varphi_n}(\omega) = \frac{1}{B\lambda_n} \int_{-1}^1 e^{-i2\pi B\omega t} \epsilon_{\varphi_n}(t) dt$$

Because $\mu_n = B|\lambda_n|^2$, by (3.36),

$$(3.46) \quad \max_{t \in [-1, 1]} |\varepsilon_{\varphi_n}(t)| \leq \frac{2}{|\lambda_n|} \max_{t \in [-1, 1]} |\epsilon_{\varphi_n}(t)|$$

$$(3.47) \quad \leq \frac{2\sqrt{B}}{\mu_n^{3/2}} \max_{t \in [-2, 2]} |\epsilon_B(2\pi t)|$$

Similar to the method of [1], (3.43) can be used to build approximate PSWF by first solving the eigensystem

$$(3.48) \quad \varphi_n(\omega_m) = \frac{1}{B\mu_n} \sum_{k=-M}^M \alpha_k 2B \operatorname{sinc}(2\pi B(\omega_m - \omega_k)) \varphi_n(\omega_k)$$

for the eigenvector $\varphi_n(\omega_k)$, followed by substituting $\varphi_n(\omega_k)$ back in (3.43):

$$(3.49) \quad \varphi_n(t) = \frac{1}{B\mu_n} \sum_{k=-M}^M \alpha_k 2B \operatorname{sinc}(2\pi B(t - \omega_k)) \varphi_n(\omega_k) + \varepsilon_{\varphi_n}(t),$$

where $\varepsilon_{\varphi_n}(\omega_m) = 0$, for $m = -M, \dots, M$. The eigenvectors $\phi_n(\omega_k)$ are generalizations of discrete prolate spheroidal sequences (DPSS) [23]. When ω_k are uniformly

sampled they are equivalent to DPSS, which asymptotically approximate PSWF [23]. Similar to the discussion in Section 3.2.2, we say the eigensystem (3.48) provides an approximation to PSWF. Because it can only capture $2M + 1$ of the eigenvalues, which we denote by $\mu_{n=0,\dots,2M}$, by (3.27), one shall choose $M \geq \lceil 2B - 1/2 \rceil$ in order to capture all the eigenvalues close to one and some of the eigenvalues in the transition zone from one to zero, depending on the desired accuracy of the approximation.

Example 6. Consider the quadratures of discrete inverse Fourier transform for $B = \frac{2M+1}{4}$

$$(3.50) \quad (\alpha_m, \omega_m)_{m=-M}^M = \left(\frac{1}{2}, \frac{2m}{2M+1} \right)_{m=-M}^M$$

for some positive integer M . Then (3.43) becomes

$$(3.51) \quad \varphi_n(t) = \frac{1}{\mu_n} \sum_{k=-M}^M \operatorname{sinc} \left(\pi \left[\frac{2M+1}{2} t - k \right] \right) \varphi_n \left(\frac{2k}{2M+1} \right) + \varepsilon_{\varphi_n}(t)$$

Consequently, the eigensystem for approximate PSWF is

$$(3.52) \quad \begin{aligned} \varphi_n \left(\frac{2m}{2M+1} \right) &= \frac{1}{\mu_n} \sum_{k=-M}^M \operatorname{sinc}(\pi[m-k]) \varphi_n \left(\frac{2k}{2M+1} \right) \\ &= \frac{1}{\mu_n} \sum_{k=-M}^M \delta_{m,k} \varphi_n \left(\frac{2k}{2M+1} \right) \\ &= \frac{1}{\mu_n} \varphi_n \left(\frac{2m}{2M+1} \right) \end{aligned}$$

for $m = -M, \dots, M$ which implies that $\mu_n = 1$ for $n = 0, \dots, 2M$. As mentioned above, $\varphi_n \left(\frac{2m}{2M+1} \right)$ are referred to as discrete prolate spheroidal sequences and were studied in [23] along with their relationship to periodic discrete prolate spheroidal sequences (P-DPSS). This example shows that, similar to P-DPSS [28], eigenvalues of DPSS are not necessarily simple and therefore definition of DPSS can be non unique.

3.3. Discrete convolution representation of band-limited approximation of compactly supported functions.

Theorem 7. Consider a function $f(t)$ compactly supported on $t \in [-1, 1]$. Its band-limited projection $f_B(t)$ can be computed by

$$(3.53) \quad f_B(t) = \sum_{k=-M}^M 2B \operatorname{sinc}(2\pi B(t - \omega_k)) f_k + \epsilon_{f_B}(t)$$

where

$$(3.54) \quad f_k = \sum_{m=-M}^M f(\omega_m) \alpha_m R_m(\omega_k)$$

and (α_m, ω_m) satisfy (3.7) and

$$(3.55) \quad R_m(t) = \sum_{n=0}^{2M} \mu_n^{-1} \varphi_n(\omega_m) \varphi_n(t)$$

Proof. Substituting (3.43) in (3.33), we obtain

$$(3.56) \quad f_B(t) = \sum_{k=-M}^M \alpha_k 2B \operatorname{sinc}(2\pi B(t - \omega_k)) \tilde{f}_B(\omega_k) + \epsilon_{f_B}(t)$$

where

$$(3.57) \quad \tilde{f}_B(t) = \frac{1}{B} \sum_{n=0}^{2M} f_{B,n} \varphi_n(t)$$

$$(3.58) \quad \epsilon_{f_B}(t) = \sum_{n=0}^{2M} \mu_n f_{B,n} \varepsilon_{\varphi_n}(t)$$

with $f_{B,n}$ defined in (3.29). Similarly, substituting (3.43) in (3.29), we obtain

$$(3.59) \quad f_{B,n} = \frac{1}{B\mu_n} \sum_{k=-M}^M \alpha_k \varphi_n(\omega_k) f_B(\omega_k) + \frac{1}{\mu_n} \int_{-1}^1 f_B(t) \varepsilon_{\varphi_n}(t) dt,$$

and substituting (3.59) in (3.57), we obtain

$$(3.60) \quad \tilde{f}_B(t) = \frac{1}{B^2} \sum_{m=-M}^M \alpha_m f_B(\omega_m) R_m(t) + \sum_{n=0}^{2M} \varphi_n(t) \left(\int_{-\infty}^{\infty} f_B(\tau) \varepsilon_{\varphi_n}(\tau) d\tau \right).$$

□

Corollary 8. *The error $\epsilon_{f_B}(t)$, for $t \in [-1, 1]$ is bounded by*

$$(3.61) \quad \max_{t \in [-1, 1]} |\epsilon_{f_B}(t)| \leq C \max_{t \in [-1, 1]} |f_B(t)| \max_{t \in [-2, 2]} |\epsilon_B(2\pi t)|$$

for some constant C .

Proof. By (3.58), for $t \in [-1, 1]$

$$(3.62) \quad \begin{aligned} \max_{t \in [-1, 1]} |\epsilon_{f_B}(t)| &\leq \sum_{n=0}^{2M} \mu_n |f_{B,n}| |\varepsilon_{\varphi_n}(t)| \\ &\leq \sum_{n=0}^{2M} \mu_n |f_{B,n}| 2\sqrt{B} \mu_n^{-3/2} \max_{t \in [-2, 2]} |\epsilon_B(2\pi t)| \end{aligned}$$

where we used (3.47) to write the second inequality. By (3.59) and (3.47), because $\alpha_k \in \mathbb{R}^+$, we have

$$(3.63) \quad \begin{aligned} |f_{B,n}| &\leq \mu_n^{-1} \max_{t \in [-1, 1]} |f_B(t)| \left[B^{-1} \sum_{k=-M}^M \alpha_k + 4\sqrt{B} \mu_n^{-1/2} \max_{t \in [-2, 2]} |\epsilon_B(2\pi t)| \right] \\ &= \mu_n^{-1} \max_{t \in [-1, 1]} |f_B(t)| \left[B^{-1} (2B - \epsilon_B(0)) + 4\sqrt{B} \mu_n^{-1/2} \max_{t \in [-2, 2]} |\epsilon_B(2\pi t)| \right] \end{aligned}$$

where we used the fact that $\sum_{k=-M}^M \alpha_k = 2B - \epsilon_B(0)$ by (3.7), $\varphi_n(\omega_m)$ are eigenvector obtained by solving (3.48), hence have unit norm, i.e. $\sum_m |\varphi_n(\omega_m)|^2 = 1$, and $\max_m |\varphi_n(\omega_m)| \leq 1$. Then

$$(3.64) \quad \max_{t \in [-1, 1]} |\epsilon_{f_B}(t)| \leq C \max_{t \in [-2, 2]} |\epsilon_B(2\pi t)| \max_{t \in [-1, 1]} |f_B(t)|$$

where the constant C is given by

$$(3.65) \quad C = \sum_{n=0}^{2M} \left[\begin{array}{l} 2B^{-1/2} \mu_n^{-3/2} (2B - \epsilon_B(0)) \\ + 8B \mu_n^{-2} \max_{t \in [-2, 2]} |\epsilon_B(2\pi t)| \end{array} \right].$$

□

Example 9. Considering the quadratures $(\alpha_m, \omega_m) = \left(\frac{2B}{2M+1}, \frac{2m}{2M+1} \right)_{m=-M}^M$ of the discrete inverse Fourier transform for fixed B , $\mu_n = 1$ and, by (B.26)³, $\epsilon_B(0) = 0$. Then, using (3.56) and Corollary 8, the error between the nodes is bounded by

$$(3.66) \quad \begin{aligned} |\epsilon_{f_B}(t)| &\leq \left[\begin{array}{l} \max_{t \in [-1, 1]} |f_B(t)| \max_{t \in [-2, 2]} |\epsilon_B(2\pi t)| \\ \times \sum_{n=0}^{2M} [4B^{1/2} + 8B \max_{t \in [-2, 2]} |\epsilon_B(2\pi t)|] \end{array} \right] \\ &= \left[\begin{array}{l} \max_{t \in [-1, 1]} |f_B(t)| \max_{t \in [-2, 2]} |\epsilon_B(2\pi t)| \\ \times (2M+1) [4B^{1/2} + 8B \max_{t \in [-2, 2]} |\epsilon_B(2\pi t)|] \end{array} \right] \end{aligned}$$

for $t \in [-1, 1]$. By (B.27), one can achieve $\max_{t \in [-2, 2]} |\epsilon_B(2\pi t)| = \mathcal{O}\left((2M+1)^{-2}\right)$ consequently $|\epsilon_{f_B}(t)| \leq \max_{t \in [-1, 1]} |f_B(t)| \mathcal{O}\left((2M+1)^{-1}\right)$ which is in the order of the truncation errors presented in Section VI of [13].

4. R -LIMITED FUNCTIONS

In this section we introduce an equivalent of R -limited functions with respect to a linear transformation and R -Slepian functions which are multivariate generalization of band-limited functions and prolate spheroidal wave functions, respectively. Then we prove the generalizations of Theorems 1 and 7 to R -limited functions.

Let $GL(\mathbb{R}, N)$ denote the general linear group, the set of invertible matrices in $\mathbb{R}^{N \times N}$, and

$$R_A = \{\mathbf{k} = A\mathbf{x} \mid \mathbf{x} \in R \subset \mathbb{R}^N, A \in GL(\mathbb{R}, N)\}$$

for some compact $R \subset \mathbb{R}^N$. Employing the terminology introduced in [22], we define R_B -limited functions by

$$(4.1) \quad f_B(\mathbf{x}) = \int_{R_B} \hat{f}_B(\mathbf{k}) e^{i2\pi \mathbf{k} \cdot \mathbf{x}} d\mathbf{k}$$

where $B \in GL(\mathbb{R}, N)$ is a real symmetric matrix and

$$(4.2) \quad \hat{f}_B(\mathbf{k}) = \int_{\mathbb{R}^N} f_B(\mathbf{x}) e^{-i2\pi \mathbf{k} \cdot \mathbf{x}} d\mathbf{x}.$$

Here B is a multidimensional analogue of band-limit. When B is the identity matrix, $R_I = R$, one obtains definition of R -limited functions of [22].

³ $\lim_{x \rightarrow 0} \text{sinc}(Bx) = \lim_{x \rightarrow 0} \frac{\sin(Bx)(2M+1)^{-1}}{\sin(Bx(2M+1)^{-1})} = 1$

Alternatively, we can write

$$\begin{aligned}
 f_B(\mathbf{x}) &= \int_{R_B} \int_{\mathbb{R}^N} f_B(\mathbf{y}) e^{i2\pi\mathbf{k}\cdot(\mathbf{x}-\mathbf{y})} d\mathbf{y} d\mathbf{k} \\
 &= \int_{\mathbb{R}^N} f_B(\mathbf{y}) \left[|\det(B)| \int_R e^{i2\pi B\mathbf{k}\cdot(\mathbf{x}-\mathbf{y})} d\mathbf{k} \right] d\mathbf{y} \\
 (4.3) \quad &= \int_{\mathbb{R}^N} f_B(\mathbf{y}) |\det(B)| K(2\pi B(\mathbf{x}-\mathbf{y})) d\mathbf{y}
 \end{aligned}$$

where $\det(B)$ denotes the determinant of B and

$$(4.4) \quad K(\mathbf{x}) = \int_R e^{i\mathbf{k}\cdot\mathbf{x}} d\mathbf{k}.$$

Given a function $f(\mathbf{x})$, its R_B -limited projection $P_B[f](\mathbf{x})$, denoted by $f_B(\mathbf{x})$ for short, is defined by

$$(4.5) \quad P_B[f](\mathbf{x}) = f_B(\mathbf{x}) = \int_{R_B} \hat{f}(\mathbf{k}) e^{i2\pi\mathbf{k}\cdot\mathbf{x}} d\mathbf{k}$$

or, equivalently, in the convolution representation using convolution theorem

$$(4.6) \quad P_B[f](\mathbf{x}) = \int_{\mathbb{R}^N} f(\mathbf{y}) |\det(B)| K(2\pi B(\mathbf{x}-\mathbf{y})) d\mathbf{y}.$$

Note that $\hat{f}_B(\mathbf{k}) = \hat{f}(\mathbf{k})$, for $\mathbf{k} \in R_B$.

4.1. Discrete Fourier representation of R -limited approximation of compactly supported functions.

Theorem 10. Consider a discretization of the integral representation (4.4) of $K(\mathbf{x})$

$$(4.7) \quad |\det(B)| K(B\mathbf{x}) = \sum_m \alpha_m e^{i\mathbf{k}_m \cdot B\mathbf{x}} + \epsilon_K(\mathbf{x})$$

for $\mathbf{k}_m \in R$. For a function $f(\mathbf{x})$ compactly supported within a region $X \subset \mathbb{R}^n$, its R -limited projection can be approximated by

$$(4.8) \quad f_B(\mathbf{x}) = \sum_m \alpha_m e^{i2\pi B\mathbf{k}_m \cdot \mathbf{x}} \hat{f}(B\mathbf{k}_m) + \epsilon_f(\mathbf{x})$$

and (4.8) provides a discretization of (4.1) with

$$(4.9) \quad \max_{\mathbf{x} \in X} |\epsilon_f(\mathbf{x})| \leq |X| \max_{\mathbf{x} \in X} |f(\mathbf{x})| \max_{\mathbf{x} \in X+X} |\epsilon_K(2\pi\mathbf{x})|,$$

where $X+X = \{\mathbf{x} | \mathbf{x} = \mathbf{x}_1 + \mathbf{x}_2, \mathbf{x}_1, \mathbf{x}_2 \in X\}$ and $|X| = \int_X d\mathbf{x}$.

Proof. Substituting (4.7) into (4.6), we obtain (4.8) where

$$(4.10) \quad \epsilon_f(\mathbf{x}) = \int_X f(\mathbf{y}) \epsilon_K(2\pi[\mathbf{x}-\mathbf{y}]) d\mathbf{y}.$$

□

For $f_B(\mathbf{x})$ to accurately approximate the compactly supported function $f(\mathbf{x})$ over $\mathbf{x} \in X$, by (4.9), one needs to build up an approximation of $K(B\mathbf{x})$ that is accurate over the set $2\pi(X+X) = \{2\pi\mathbf{y} | \mathbf{y} \in X+X\}$.

4.2. R -Slepian functions: A multivariate generalization of PSWF. We can generalize the PSWF and their approximations presented in Sections 3.2.2 and 3.2.3 to multiple-variables to define R -Slepian functions and construct their approximations.

4.2.1. R -Slepian functions. Consider the R_B -limited projection of a compactly supported function with support $S \in \mathbb{R}^N$:

$$(4.11) \quad P_B[f](\mathbf{x}) = f_B(\mathbf{x}) = \int_S f(\mathbf{y}) |\det(B)| K(2\pi B(\mathbf{x} - \mathbf{y})) d\mathbf{y}$$

restricted to $\mathbf{x} \in S$. $P_B[f](\mathbf{x})$ is a positive definite operator. Furthermore, if R is symmetric, i.e. $R = -R = \{-\mathbf{x} | \mathbf{x} \in R\}$, then $K(\mathbf{x}) = K(-\mathbf{x})$ is real,

$$(4.12) \quad K(\mathbf{x}) = \int_R \cos(\mathbf{k} \cdot \mathbf{x}) d\mathbf{k},$$

P_B is a positive definite real symmetric operator,

$$(4.13) \quad \begin{aligned} & \int_S \int_S f(\mathbf{y}) |\det(B)| K(2\pi B(\mathbf{x} - \mathbf{y})) d\mathbf{y} f(\mathbf{x}) d\mathbf{x} \\ &= \int_S \int_S f(\mathbf{y}) |\det(B)| K(2\pi B(\mathbf{y} - \mathbf{x})) d\mathbf{y} f(\mathbf{x}) d\mathbf{x} \\ &= \int_{R_B} |\hat{f}(\mathbf{k})|^2 d\mathbf{k} \geq 0, \end{aligned}$$

and, consequently, by Mercer's theorem (see page 245 [21]), accepts a discrete eigendecomposition

$$(4.14) \quad \mu_n \varphi_n(\mathbf{x}) = \int_S \varphi_n(\mathbf{y}) |\det(B)| K(2\pi B(\mathbf{x} - \mathbf{y})) d\mathbf{y}$$

with positive eigenvalues μ_n and real eigenfunctions $\varphi_n(\mathbf{x}) \in \mathbb{R}$ for $\mathbf{x} \in S$. We refer to eigenfunctions $\varphi_n(\mathbf{x})$ as the R -Slepian functions. For the sake of simplicity of the discussion we will consider symmetric R . The case of non-symmetric R can be reduced to the symmetric case by translation of R away from the origin to exclude origin and consider $R \cup -R$.

Consider, $S = R$ and solutions $\psi(\mathbf{x})$ of the equation

$$(4.15) \quad \lambda \psi(\mathbf{x}) = \int_R \psi(\mathbf{k}) e^{i2\pi B\mathbf{k} \cdot \mathbf{x}} d\mathbf{k}, \quad \mathbf{x} \in R$$

Define $\psi_e(\mathbf{x}) = [\psi(\mathbf{x}) + \psi(-\mathbf{x})]/2$ and $\psi_o(\mathbf{x}) = [\psi(\mathbf{x}) - \psi(-\mathbf{x})]/2$ as the even and odd parts of $\psi(\mathbf{x})$. For symmetric R , i.e. $R = -R$, we have

$$(4.16) \quad \begin{aligned} \lambda [\psi_e(\mathbf{x}) + \psi_o(\mathbf{x})] &= \int_R \psi(\mathbf{k}) e^{i2\pi B\mathbf{k} \cdot \mathbf{x}} d\mathbf{k} \\ &= \left\{ \begin{array}{l} \int_R \psi_e(\mathbf{k}) \cos(2\pi B\mathbf{k} \cdot \mathbf{x}) d\mathbf{k} \\ +i \int_R \psi_o(\mathbf{k}) \sin(2\pi B\mathbf{k} \cdot \mathbf{x}) d\mathbf{k} \end{array} \right\} \end{aligned}$$

Considering the equations

$$(4.17) \quad \beta_e \psi_e(\mathbf{x}) = \int_R \psi_e(\mathbf{k}) \cos(2\pi B\mathbf{k} \cdot \mathbf{x}) d\mathbf{k}$$

$$(4.18) \quad \beta_o \psi_o(\mathbf{x}) = \int_R \psi_o(\mathbf{k}) \sin(2\pi B\mathbf{k} \cdot \mathbf{x}) d\mathbf{k},$$

which have real symmetric kernel with real eigenvalues and eigenfunctions, the real and imaginary eigenvalues of (4.15) are associated with eigenfunctions of (4.17) and (4.18), respectively. Completeness follow from Fourier theory using the same arguments as in [22, 21].

Eigenfunctions $\varphi_n(\mathbf{x})$ of (4.15),

$$(4.19) \quad \lambda_n \varphi_n(\mathbf{x}) = \int_R \varphi_n(\mathbf{k}) e^{i2\pi B\mathbf{k}\cdot\mathbf{x}} d\mathbf{k}, \quad \mathbf{x} \in R,$$

are also eigenfunctions of (4.14):

$$(4.20) \quad \begin{aligned} & \int_R \varphi_n(\mathbf{y}) |\det(B)| K(2\pi B(\mathbf{x} - \mathbf{y})) d\mathbf{y} \\ &= |\det(B)| \int_R e^{i2\pi B\mathbf{x}\cdot\mathbf{k}} \left[\int_R \varphi_n(\mathbf{y}) e^{-i2\pi B\mathbf{y}\cdot\mathbf{k}} d\mathbf{y} \right] d\mathbf{k} \\ &= \bar{\lambda}_n |\det(B)| \int_R e^{i2\pi B\mathbf{x}\cdot\mathbf{k}} \varphi_n(\mathbf{k}) d\mathbf{k} \\ &= |\lambda_n|^2 |\det(B)| \varphi_n(\mathbf{x}) \end{aligned}$$

with

$$(4.21) \quad \mu_n = |\det(B)| |\lambda_n|^2.$$

Similar to the case of PSWF, R -Slepian functions satisfy double orthogonality relation [22]

$$(4.22) \quad \mu_n \int_{\mathbb{R}^N} \varphi_n(\mathbf{x}) \varphi_m(\mathbf{x}) d\mathbf{x} = \int_R \varphi_n(\mathbf{x}) \varphi_m(\mathbf{x}) d\mathbf{x} = \delta_{m,n}$$

4.2.2. *Approximating R -Slepian functions as eigenfunction of $e^{i2\pi B\mathbf{k}_m \cdot \mathbf{x}_l}$.* Similar to the single dimensional case, if one can build up an approximation to (4.12) or, equivalently, (4.4),

$$(4.23) \quad K(\mathbf{x}) = \sum_{m=1}^M \alpha_m \exp(i\mathbf{k}_m \cdot \mathbf{x}) + \epsilon_K(\mathbf{x})$$

for some $\mathbf{k}_m \in R$, then, substituting (4.23) in (4.14), we obtain

$$(4.24) \quad \lambda_n \varphi_n(\mathbf{x}) = \sum_{m=1}^M \alpha_m e^{i2\pi B\mathbf{k}_m \cdot \mathbf{x}} \varphi_n(\mathbf{k}_m) + \epsilon_{\varphi_n}(\mathbf{x})$$

where

$$(4.25) \quad \epsilon_{\varphi_n}(\mathbf{x}) = \int_R \varphi_n(\mathbf{y}) \epsilon_K(2\pi B[\mathbf{x} - \mathbf{y}]).$$

We can approximate R -Slepian functions by substituting the eigenvectors $\varphi_n(\mathbf{x}_l)$ of the equation

$$(4.26) \quad \lambda_n \varphi_n(\mathbf{x}_l) = \sum_{m=1}^M \alpha_m e^{i2\pi B\mathbf{k}_m \cdot \mathbf{x}_l} \varphi_n(\mathbf{k}_m), \quad \mathbf{x}_l \in \bigcup_m \{\mathbf{k}_m\}$$

into (4.24) for $n, l = 1, \dots, M$.

Because there are $|\det(B)| |S| |R|$ number of eigenvalues μ_n close to one (see Theorem 3 in [16]⁴), in order to capture all the eigenvalues close to one, one shall

⁴Recently this theorem is rediscovered in [8].

have $M \geq \lceil |\det(B)| |S| |R| \rceil$. A detailed analysis of the characterization of the eigenvalues of the projection operator defined in (4.11) around one, zero and the transition zone can be found in [25].

4.2.3. *Approximating R -Slepian functions as eigenfunction of $K(2\pi B[\mathbf{k}_m - \mathbf{k}_l])$.* Multiplying both sides of (4.24) by $|\det(B)| e^{-i2\pi B\mathbf{k}\cdot\mathbf{x}}$, integrating over \mathbf{x} and using (4.21), we obtain

$$(4.27) \quad \begin{aligned} |\lambda_n|^2 |\det(B)| \varphi_n(\mathbf{k}) &= \mu_n \varphi_n(\mathbf{k}) \\ &= \sum_{m=1}^M \alpha_m |\det(B)| K(2\pi B[\mathbf{k} - \mathbf{k}_m]) \varphi_n(\mathbf{k}_m) + \varepsilon_{\varphi_n}(\mathbf{k}) \end{aligned}$$

where

$$(4.28) \quad \varepsilon_{\varphi_n}(\mathbf{k}) = \int_R \varepsilon_{\varphi_n}(\mathbf{x}) e^{-i2\pi B\mathbf{k}\cdot\mathbf{x}} d\mathbf{x}$$

Consequently, by (4.27), we can approximate R -Slepian functions by substituting the eigenvectors $\varphi_n(\mathbf{k}_m)$ of the equation

$$(4.29) \quad \mu_n \varphi_n(\mathbf{k}_l) = \sum_{m=1}^M \alpha_m |\det(B)| K(2\pi B[\mathbf{k}_l - \mathbf{k}_m]) \varphi_n(\mathbf{k}_m)$$

for $n = 1, \dots, M$.

4.3. Discrete convolution representation of R -limited approximation of compactly supported functions. Using R -Slepian functions, we can prove a generalization of the sampling and interpolation theorem, Theorem 7, for R_A -limited functions. To do this, we first show the sampling theorem of R_B -limited functions for symmetric B and then generalize it to R_A -functions for an arbitrary $A \in GL(N, \mathbb{R})$.

Lemma 11. *Given a symmetric $B \in GL(N, \mathbb{R})$, i.e. $B = B^T$ and a function $f(\mathbf{x})$, R_B -limited projection $f_B(\mathbf{x})$ of $f(\mathbf{x})$ can be approximated by*

$$(4.30) \quad f_B(\mathbf{x}) \approx \sum_{m=1}^M f_m |\det(B)| K(2\pi B(\mathbf{x} - \mathbf{k}_m))$$

where

$$(4.31) \quad f_m = \sum_{n=1}^M f_B(\mathbf{k}_n) \alpha_n |\det(B)| K(2\pi B(\mathbf{k}_m - \mathbf{k}_n)) \alpha_n.$$

Proof. Consider a symmetric $B \in GL(N, \mathbb{R})$. Because $\varphi_n(\mathbf{x})$ are complete for compactly supported functions as well as R_B -limited functions, we can expand any R_B -limited function f_B using (4.27) as follows:

$$(4.32) \quad \begin{aligned} f_B(\mathbf{x}) &= \int_R f(\mathbf{x}) |\det(B)| K(2\pi B(\mathbf{x} - \mathbf{y})) \\ &= \sum_{n=1}^M \mu_n f_{B,n} \varphi_n(\mathbf{x}) \\ &= \left\{ \begin{aligned} &\sum_{m=1}^M \alpha_m |\det(B)| K(2\pi B(\mathbf{x} - \mathbf{k}_m)) \tilde{f}_B(\mathbf{k}_m) \\ &+ \sum_{n=1}^M \mu_n f_{B,n} \varepsilon_{\varphi_n}(\mathbf{x}) \end{aligned} \right\} \end{aligned}$$

where

$$(4.33) \quad \tilde{f}_B(\mathbf{k}) = \sum_{n=1}^M f_{B,n} \varphi_n(\mathbf{k})$$

(4.33) is a multivariate generalization of (3.33)

We rewrite $f_{B,n}$ as

$$(4.34) \quad f_{B,n} = \frac{1}{\mu_n} \sum_{m=1}^M \alpha_m \varphi_n(\mathbf{k}_m) f_B(\mathbf{k}_m) + \int_{\mathbb{R}^N} f_B(\mathbf{x}) \varepsilon_{\varphi_n}(\mathbf{x}) d\mathbf{x}.$$

Substituting (4.34) in (4.33), we have

$$(4.35) \quad \tilde{f}_B(\mathbf{k}) = \sum_{m=1}^M \alpha_m f_B(\mathbf{k}_m) R_m(\mathbf{k}) + \left(\sum_{n=1}^M \varphi_n(\mathbf{k}) \int_{\mathbb{R}^N} f_B(\mathbf{x}) \varepsilon_{\varphi_n}(\mathbf{x}) d\mathbf{x} \right)$$

where

$$(4.36) \quad R_m(\mathbf{k}) = \sum_{n=1}^M \frac{1}{\mu_n} \varphi_n(\mathbf{k}_m) \varphi_n(\mathbf{k}).$$

Similar to the single dimensional case, a regularized approximation to $R_m(\mathbf{k})$ is given by $|\det(B)| K(2\pi B(\mathbf{k} - \mathbf{k}_m))$, leading to the approximate interpolation formula

$$(4.37) \quad f_B(\mathbf{x}) \approx \sum_{m=1}^M \left\{ \alpha_m |\det(B)| K(2\pi B(\mathbf{x} - \mathbf{k}_m)) \times \left[\sum_{n=1}^M \alpha_n f_B(\mathbf{k}_n) |\det(B)| K(2\pi B(\mathbf{k}_m - \mathbf{k}_n)) \right] \right\}$$

□

Theorem 12. Consider the R_A -limited function

$$(4.38) \quad f_A(\mathbf{x}) = \int_{AR} f(\mathbf{y}) |\det(A)| K(2\pi A^T(\mathbf{x} - \mathbf{y})) d\mathbf{y}$$

for some, not necessarily symmetric, $A \in GL(N, \mathbb{R})$. Then

$$(4.39) \quad f_A(\mathbf{x}) = \sum_m \alpha_m |\det(B)| K(2\pi A^T(\mathbf{x} - A\mathbf{k}_m)) \tilde{f}_A(A\mathbf{k}_m) + \sum_n \mu_n g_{B,n} \varepsilon_{\varphi_n}(A^{-1}\mathbf{x}), \quad \mathbf{x} \in \mathbb{R}^N, A\mathbf{k}_m \in R_A$$

where $\tilde{f}_A(A\mathbf{k}_m)$ and $g_{B,n}$ are defined by (4.44) and (4.43), respectively.

Proof. Let $B = A^T A$. Then $g_B(\mathbf{x}) = f_A(A\mathbf{x})$ is an R_B -limited projection of $g(\mathbf{x}) = f(A\mathbf{x})$:

$$(4.40) \quad \begin{aligned} f_A(A\mathbf{x}) &= \int_R f(A\mathbf{y}) |\det(A)|^2 K(2\pi A^T(A\mathbf{x} - A\mathbf{y})) d\mathbf{y} \\ &= \int_R f(A\mathbf{y}) |\det(B)| K(2\pi B(\mathbf{x} - \mathbf{y})) d\mathbf{y} \\ g_B(\mathbf{x}) &= \int_R g(\mathbf{y}) |\det(B)| K(2\pi B(\mathbf{x} - \mathbf{y})) d\mathbf{y} \end{aligned}$$

which, by (4.32), can be approximated by

$$(4.41) \quad g_B(\mathbf{x}) = \sum_m \alpha_m |\det(B)| K(2\pi B(\mathbf{x} - \mathbf{k}_m)) \tilde{g}_B(\mathbf{k}_m) \\ + \sum_n \mu_n g_{B,n} \varepsilon_{\varphi_n}(\mathbf{x}), \quad \mathbf{x} \in \mathbb{R}^N, \mathbf{k}_m \in R.$$

or equivalently

$$(4.42) \quad f_A(\mathbf{x}) = \sum_m \alpha_m |\det(B)| K(2\pi A^T(\mathbf{x} - A\mathbf{k}_m)) \tilde{f}_A(A\mathbf{k}_m) \\ + \sum_n \mu_n g_{B,n} \varepsilon_{\varphi_n}(A^{-1}\mathbf{x}), \quad \mathbf{x} \in \mathbb{R}^N, A\mathbf{k}_m \in R_A.$$

Here

$$(4.43) \quad g_{B,n} = \int_{\mathbb{R}^N} f_A(A\mathbf{x}) \varphi_n(\mathbf{x}) d\mathbf{x} \\ = \frac{1}{\det(A)} \int_{\mathbb{R}^N} f_A(\mathbf{x}) \varphi_n(A^{-1}\mathbf{x}) d\mathbf{x} \\ = \int_R f_A(A\mathbf{x}) \varphi_n(\mathbf{x}) d\mathbf{x} \\ = \frac{1}{\mu_n} \left\{ \sum_{m=1}^M \alpha_m f_A(A\mathbf{k}_m) \varphi_n(\mathbf{k}_m) + \int_R f_A(A\mathbf{x}) \varepsilon_{\varphi_n}(\mathbf{x}) d\mathbf{x} \right\},$$

and

$$(4.44) \quad \tilde{f}_A(A\mathbf{k}) = \tilde{g}_B(\mathbf{k}) = \sum_n g_{B,n} \varphi_n(\mathbf{k})$$

with $\varphi_n(\mathbf{x})$ being the eigenvector of the projection operator P_B with respect to the symmetric matrix B . \square

4.4. Construction of discrete Fourier approximation of the kernel (4.7). It is important to note that both Theorems 10 and 12 rely on finding an approximation of the convolution kernel in the form of (4.23). Although there is no unique way of finding an approximation in the form of (4.23), it can be constructed using tools from approximation theory. Considering that two and three dimensional domains can be approximated using tetrahedral and triangular meshes along with their multidimensional extensions [4, 18], it is necessary to build quadrature (α_m, \mathbf{k}_m) to approximate triangle-limited and tetrahedral-limited (shortly T -limited) functions. Because our results do not require R_A to be connected, and they can be generalized to $R_A = \cup_{l=1}^L A_l R_l$ where $A_l \in GL(\mathbb{R}^N)$ and $R_l \subset \mathbb{R}^N$ such that intersection of $\{A_l R_l\}_{l=1}^L$ has measure zero, i.e. $|\cap_{l=1}^L A_l R_l| = 0$, quadratures obtained for T -limited functions can be patched together to construct an approximation of the form (4.23). In this case, the convolution kernel becomes

$$(4.45) \quad K_\Sigma(\mathbf{x}) = \sum_{m=1}^M |\det(A_m)| K_m(2\pi A_m^T \mathbf{x})$$

where $K_m(\mathbf{x}) = \int_{R_m} e^{i\mathbf{k}\cdot\mathbf{x}} d\mathbf{k}$ and, consequently, the R_A -limited projection of a function is given by

$$(4.46) \quad f_A(\mathbf{x}) = \int_{\mathbb{R}^N} f(\mathbf{y}) K_\Sigma(\mathbf{x} - \mathbf{y}) d\mathbf{y} = \sum_{l=1}^L f_{A_l}(\mathbf{x})$$

where

$$(4.47) \quad f_{A_l}(\mathbf{x}) = \int_{\mathbb{R}^N} f(\mathbf{y}) |\det(A_l)| K(2\pi A_l^T(\mathbf{x} - \mathbf{y})) d\mathbf{y}.$$

By Corollary 12, because each $f_{A_l}(\mathbf{x})$ can be approximated by

$$(4.48) \quad f_{A_l}(\mathbf{x}) \approx \sum_{m_l} \alpha_{m_l} |\det(B_l)| K(2\pi A_l^T(\mathbf{x} - A_l \mathbf{k}_{m_l, l})) \tilde{g}_{B_l}(\mathbf{k}_{m_l, l}) \\ + \sum_{m_l} \mu_{m_l} g_{B, m_l} \varepsilon_{\varphi_{m_l}}(A_l^{-1} \mathbf{x}), \quad \mathbf{x} \in \mathbb{R}^N, A_l \mathbf{k}_{m_l, l} \in A_l R_l$$

then $f_A(\mathbf{x})$ can be approximated using samples of $f(\mathbf{x})$ for $\mathbf{x} \in \{A_l \mathbf{k}_{m_l, l}\}_{\substack{l=1, \dots, L \\ m_l=1, \dots, M_l}}$.

In Appendix C, we provide a method to construct quadratures for T -limited functions, specifically for isosceles triangle and trirectangular tetrahedron which are used to construct quadratures for equilateral triangle and regular tetrahedron, respectively, that satisfy the corresponding symmetry properties. We present two ways to construct the quadrature for equilateral triangle, one capturing the symmetries of the triangle and the other doesn't. Although approximations are constructed to capture the behavior of the kernel and its derivatives at zero, the quadrature that satisfy the symmetry properties provide a more accurate approximation within a larger vicinity of zero with fewer number of nodes.

Another special case of R -limited functions that have practical importance in multidimensional signal processing seismic data is considered in Appendix D which can also be extended to image processing in 2D and video processing 3D. We present the convolution kernels and construction of corresponding quadratures that can be used in sampling and interpolation Theorems 10 and 12 in Appendix D.

5. CONCLUSION

In this manuscript, we proved duality between the discretization of Fourier and convolution representations of R -limited functions which lead to the sampling and interpolation theorem, Theorem 12, where the interpolation is to be understood as an approximation within a desired accuracy over a compact region. Because discretization of the Fourier representation is over a compact support, so is the discretization of the convolution representation. Thus, an R -limited function can be approximated from samples over a compact support that is similar to R . We provided examples of convolution kernels for some special cases of R -limited functions, namely T -limited and C -limited functions whose Fourier transforms are supported in a triangle, or tetrahedron, and cone, respectively. We constructed discretization of the Fourier representation of these kernels which can be used along with sampling and interpolation theorems.

ACKNOWLEDGMENTS

I would like to thank Lucas Monzon who introduced moment problems and quadrature methods to me. He has been a mentor, a colleague and most importantly a dear friend. Initial sketches of results in Sections 3.2.3 and 4.2.3 were obtained with him in 2012. He also reviewed the manuscript in detail which made the content more accurate and clearer. Our collaboration wouldn't have been possible without support and trust of Konstantin Osypov. I would like to thank Kemal Özdemir for extensive discussions during the final preparation of this manuscript and his invaluable signal processing perspective. I would like to thank Ozan Öktem and Daan Huybrechs for giving me the opportunity to present parts of this work at KTH Royal Institute of Technology and University of Leuven where follow up questions, comments and discussions have improved the flow and content of the manuscript. Finally I thank Garret Flagg and Vladimir Druskin for reading the initial draft of the manuscript and providing constructive feedback.

REFERENCES

- [1] G. Beylkin and L. Monzón. On generalized Gaussian quadratures for exponentials and their applications. *Applied and Computational Harmonic Analysis*, 12(3):332–373, 2002.
- [2] William L Briggs et al. *The DFT: An Owners' Manual for the Discrete Fourier Transform*. SIAM, 1995.
- [3] Emmanuel J Candes. Multiscale chirplets and near-optimal recovery of chirps. Technical report, Technical Report, Stanford University, 2002.
- [4] Siu-Wing Cheng, Tamal K Dey, and Jonathan Shewchuk. *Delaunay mesh generation*. CRC Press, 2012.
- [5] AJW Duijndam and MA Schonewille. Nonuniform fast fourier transform. *Geophysics*, 64(2):539–551, 1999.
- [6] Alok Dutt and Vladimir Rokhlin. Fast fourier transforms for nonequispaced data. *SIAM Journal on Scientific computing*, 14(6):1368–1393, 1993.
- [7] Alan Edelman, Peter McCorquodale, and Sivan Toledo. The future fast fourier transform? *SIAM Journal on Scientific Computing*, 20(3):1094–1114, 1998.
- [8] Massimo Franceschetti. On Landau's eigenvalue theorem and information cut-sets. *Information Theory, IEEE Transactions on*, 61(9):5042–5051, 2015.
- [9] F.G. Friedlander and M.S. Joshi. *Introduction to the Theory of Distributions*. Cambridge University Press, 1998.
- [10] Walter Gautschi. Moments in quadrature problems. *Computers & Mathematics with Applications*, 33(1):105–118, 1997.
- [11] I. S. Gradshteyn and I. M. Ryzhik. *Table of integrals, series, and products*. Elsevier/Academic Press, Amsterdam, seventh edition, 2007. Translated from the Russian, Translation edited and with a preface by Alan Jeffrey and Daniel Zwillinger, With one CD-ROM (Windows, Macintosh and UNIX).
- [12] Leslie Greengard and June-Yub Lee. Accelerating the nonuniform fast fourier transform. *SIAM review*, 46(3):443–454, 2004.
- [13] Abdul J Jerri. The Shannon sampling theorem – Its various extensions and applications: A tutorial review. *Proceedings of the IEEE*, 65(11):1565–1596, 1977.
- [14] Abdul J Jerri. *The Gibbs phenomenon in Fourier analysis, splines and wavelet approximations*, volume 446. Springer Science & Business Media, 2013.
- [15] Sun-Yuan Kung. A new identification and model reduction algorithm via singular value decomposition. In *Proc. 12th Asilomar Conf. Circuits, Syst. Comput., Pacific Grove, CA*, pages 705–714, 1978.
- [16] HJ Landau. On Szegő's eigenvalue distribution theorem and non-Hermitian kernels. *Journal d'Analyse Mathématique*, 28(1):335–357, 1975.
- [17] HJ Landau and Harold Widom. Eigenvalue distribution of time and frequency limiting. *Journal of Mathematical Analysis and Applications*, 77(2):469–481, 1980.
- [18] Daniel SH Lo. *Finite Element Mesh Generation*. CRC Press, 2014.

- [19] Steve Mann and Simon Haykin. The chirplet transform: Physical considerations. *Signal Processing, IEEE Transactions on*, 43(11):2745–2761, 1995.
- [20] Andrei Osipov, Vladimir Rokhlin, and Hong Xiao. Prolate spheroidal wave functions of order zero. *Springer Ser. Appl. Math. Sci*, 187, 2013.
- [21] Frigyes Riesz and Béla Sz Nagy. *Functional analysis*. Dover Publications, 1990.
- [22] David Slepian. Prolate spheroidal wave functions, fourier analysis and uncertainty - IV: extensions to many dimensions; generalized prolate spheroidal functions. *Bell System Technical Journal*, 43(6):3009–3057, 1964.
- [23] David Slepian. Prolate spheroidal wave functions, fourier analysis, and uncertainty - V: The discrete case. *Bell System Technical Journal*, 57(5):1371–1430, 1978.
- [24] David Slepian and Henry O Pollak. Prolate spheroidal wave functions, fourier analysis and uncertainty - I. *Bell System Technical Journal*, 40(1):43–63, 1961.
- [25] A Sobolev. *Pseudo-differential operators with discontinuous symbols: Widom’s conjecture*, volume 222. American Mathematical Society, 2013.
- [26] Radomir S Stankovic, Jaakko T Astola, and Mark G Karpovsky. Some historical remarks on sampling theorem. In *Proceedings of the 2006 International TICSP Workshop on Spectral Methods and Multirate Signal Processing, SMMSP2006, Florence, Italy*, pages 2–3, 2006.
- [27] Michael Unser. Sampling-50 years after Shannon. *Proceedings of the IEEE*, 88(4):569–587, 2000.
- [28] Wen Yuan Xu and Christodoulos Chamzas. On the periodic discrete prolate spheroidal sequences. *SIAM Journal on Applied Mathematics*, 44(6):1210–1217, 1984.
- [29] Can Evren Yarman and Garret Flagg. Generalization of Padé approximation from rational functions to arbitrary analytic functions - Theory. *Math. Comp.*, 84:1835–1860, 2015.

APPENDIX A. GENERALIZATION OF PADÉ APPROXIMATION

Let $f(x)$ and $g(x)$ be two analytic functions related to each other by the Cauchy integral

$$(A.1) \quad f(x) = \int_{\Gamma} \rho(z) g(zx) dz$$

for some closed contour $\Gamma \in \mathbb{C}$ and a weighting function $\rho(z)$. A generalization of Padé approximation is achieved by finding a rational approximation to the weighting function

$$(A.2) \quad \rho(z) = \frac{1}{2\pi i} \sum_m \frac{\alpha_m}{z - \gamma_m} + \epsilon_{\rho}(z), \quad z \in \mathbb{C}$$

for some distinct $\gamma_m \in \mathbb{C}$ and error $\epsilon_{\rho}(z)$. Then we refer to

$$(A.3) \quad f(x) = \sum_m \alpha_m g(\gamma_m x) + \epsilon(x)$$

as the generalization of Padé approximation from rational function to analytic functions, for some error function $\epsilon(x)$. Substituting the power series expansion of f and g at zero into (A.1)

$$(A.4) \quad f(x) = \sum_{m=0}^{\infty} f_n x^n = \int \rho(z) \left[\sum_{m=0}^{\infty} g_n (zx)^n \right] dz$$

and equating the terms of the series, one obtains that the moments of $\rho(z)$ are given by the ratio of the power series coefficients, which we denote by h_n

$$(A.5) \quad \int \rho(z) z^n dz = h_n = \frac{f_n}{g_n} = \sum_m \alpha_m \gamma_m^n + \epsilon_n$$

for some error ϵ_n . Because (A.3) is a discrete approximation to the integral (A.1), (α_m, γ_m) are referred to as the quadratures. Individually, we refer to α_m and γ_m

$f(Bx)$	$g(x)$	f_{2n}	g_{2n}	Moment problem $h_n = \sum_m \alpha_m \gamma_m^{2n}$	Quadrature names
$\text{sinc}(Bx)$	$\cos(x)$	$\frac{(-1)^n B^{2n}}{(2n+1)!}$	$\frac{(-1)^n}{(2n)!}$	$\frac{B^{2n}}{2n+1}$	Gauss-Legendre
$J_0(Bx)$	$\cos(x)$	$\frac{(-1)^n B^{2n}}{(2^n n!)^2}$	$\frac{(-1)^n}{(2n)!}$	$\frac{(2n)! B^{2n}}{(2^n n!)^2}$	Clenshaw-Curtis
$e^{-(Bx)^2}$	$\cos(x)$	$\frac{(-1)^n B^{2n}}{n!}$	$\frac{(-1)^n}{(2n)!}$	$\frac{(2n)! B^{2n}}{n!}$	Gauss-Hermite
$\text{sinc}(Bx)$	$\exp(-x^2)$	$\frac{(-1)^n B^{2n}}{(2n+1)!}$	$\frac{(-1)^n}{n!}$	$\frac{(-1)^n B^{2n}}{(2n+1)!}$	
$J_0(Bx)$	$\text{sinc}(x)$	$\frac{(-1)^n B^{2n}}{(2^n n!)^2}$	$\frac{(-1)^n}{(2n+1)!}$	$\frac{(2n+1)! B^{2n}}{(2^n n!)^2}$	
$(Bx)^{-1} J_1(Bx)$	$x^{-1} \text{cosinc}(x)$	$\frac{(-1)^n}{2^{2n+1} n! (n+1)!}$	$\frac{(-1)^n}{(2n+2)!}$	$\frac{(2n+2)!}{2^{2n+1} n! (n+1)!}$	

TABLE 1. Example of moment problems corresponding to approximation of some even functions $f(Bx) \approx \sum_m \alpha_m g(\gamma_m x)$ in terms of other even functions $g(x)$, along with the known quadrature names (see [10]).

as weights and nodes, respectively. In [29], we presented the detailed theory of this generalization of Padé approximation and a method to compute the quadratures (α_m, γ_m) which is based on [15]. Some examples of moment problems are given in Table 1.

APPENDIX B. ON APPROXIMATIONS OF SINC

A good approximation to $\text{sinc}(x)$ within the vicinity of zero can be achieved by building up quadratures for the integral representation of $\text{sinc}(Bx)$,

$$(B.1) \quad \text{sinc}(Bx) = \frac{1}{B} \int_0^B \cos(\omega x) d\omega,$$

and then rescaling the approximation by $1/B$. One way to do this is using the method presented in Appendix A to obtain

$$(B.2) \quad \text{sinc}(Bx) = \sum_m \alpha_m \cos(\omega_m x) + \epsilon_B(x),$$

where (α_m, ω_m) satisfies the moment problem

$$(B.3) \quad h_n = \frac{f_n}{g_n} = \sum_m \alpha_m \omega_m^{2n} + \epsilon_n$$

for some small $|\epsilon_n|$ (see Figure B.2). Here

$$(B.4) \quad f_n = \frac{(-1)^n B^{2n}}{(2n+1)!}$$

and

$$(B.5) \quad g_n = \frac{(-1)^n}{(2n)!}$$

are the Taylor series coefficients of $\text{sinc}(x)$ and $\cos(x)$ at zero, respectively, and

$$(B.6) \quad \epsilon_B(x) = \sum_{n=0}^{\infty} \epsilon_n x^{2n}.$$

Solution to the moment problem is equivalent to computing Gauss-Legendre quadratures.

The approximation given in equation (B.2) yields a highly accurate approximation to the $\text{sinc}(Bx)$ in a neighborhood of zero (see Figure B.1). However, due to the rapid increase in the values of the moments h_n for large band-limit B , the construction of this approximation suffers from numerical instabilities, and therefore requires B to be in the range $0 < B \leq 2$. To overcome these challenges, approximation (B.2) can be coupled with a scaling property of the sinc, for example

$$(B.7) \quad \text{sinc}(3^n Bx) = \frac{1}{3} [2 \cos(2 \cdot 3^{n-1} Bx) + 1] \text{sinc}(3^{n-1} Bx),$$

to derive an error bound on the approximation of $\text{sinc}(3^n Bx)$ in terms of the error in the approximation to the lower bandwidth $\text{sinc}(Bx)$ as a sum of scaled cosines:

Lemma 13. *Let*

$$(B.8) \quad \epsilon_B(x) = \text{sinc}(Bx) - \sum_m \alpha_m \cos(B\theta_m x).$$

Then

$$(B.9) \quad \left| \text{sinc}(3^n Bx) - \frac{1}{3^n} \sum_m \alpha_m \sum_{k=-(3^n-1)/2}^{(3^n-1)/2} \cos((\theta_m + 2k) Bx) \right| \leq |\epsilon_B(x)|, \quad \text{for } n \geq 0.$$

Proof. We will prove by induction. For $n = 0$, this is trivial by assumption (B.8).

Let us define

$$(B.10) \quad \epsilon_{3^n B}(x) = \text{sinc}(3^n Bx) - \frac{1}{3^n} \sum_m \alpha_m \sum_{k=-(3^n-1)/2}^{(3^n-1)/2} \cos((\theta_m + 2k) Bx).$$

For $n = 1$, substituting (B.2) into the scaling property (B.7), we obtain

$$(B.11) \quad \text{sinc}(3Bx) = \frac{1}{3} \sum_m \alpha_m \sum_{k=-1}^1 \cos(B(\theta_m - 2k)x) + \frac{1}{3} [2 \cos(2Bx) + 1] \epsilon_B(x),$$

implying

$$(B.12) \quad |\epsilon_{3B}(x)| = \left| \frac{1}{3} [2 \cos(2Bx) + 1] \epsilon_B(x) \right| \leq |\epsilon_B(x)|.$$

Multiplying $\epsilon_{3^n B}(x)$ by $\frac{1}{3} [2 \cos(2 \cdot 3^n Bx) + 1]$, we have

$$(B.13) \quad \frac{1}{3} [2 \cos(2 \cdot 3^n Bx) + 1] \epsilon_{3^n B}(x) = \epsilon_{3^{n+1} B}(x)$$

which implies

$$(B.14) \quad |\epsilon_{3^{n+1} B}(x)| \leq |\epsilon_{3^n B}(x)| \leq \dots \leq |\epsilon_{3B}(x)| \leq |\epsilon_B(x)|.$$

□

Corollary 14. *The error is given by*

$$(B.15) \quad \epsilon_{3^{n+1} B}(x) = \sum_{l=-\infty}^{\infty} \text{sinc}\left(3^{n+1} B \left[x - \frac{\pi l}{B}\right]\right) \epsilon_B(x)$$

which for $x = m\pi/B$ becomes

$$(B.16) \quad \epsilon_{3^{n+1}B} \left(\frac{m\pi}{B} \right) = \epsilon_B \left(\frac{m\pi}{B} \right).$$

Furthermore,

$$(B.17) \quad \lim_{n \rightarrow \infty} 3^{n+1} 2B \epsilon_{3^{n+1}B} (x) = \sum_{l=-\infty}^{\infty} \delta \left(x - \frac{\pi l}{B} \right) \epsilon_B (x).$$

Proof. At the end of the proof of Lemma 13 we showed that the error satisfies the scaling property (B.13). Using this, we can write

$$(B.18) \quad \begin{aligned} \epsilon_{3^{n+1}B} (x) &= \frac{1}{3} [2 \cos (2 \cdot 3^n Bx) + 1] \epsilon_{3^n B} (x) \\ &= \frac{1}{3^2} [2 \cos (2 \cdot 3^{n-1} Bx) + 1] [2 \cos (2 \cdot 3^n Bx) + 1] \epsilon_{3^{n-1} B} (x) \\ &= \frac{1}{3^{n+1}} \prod_{l=1}^n [2 \cos (2 \cdot 3^l Bx) + 1] \epsilon_B (x) \end{aligned}$$

which in the Fourier domain can be written as

$$(B.19) \quad \begin{aligned} \hat{\epsilon}_{3^{n+1}B} (k) &= \frac{1}{3^{n+1}} \left(\ast_{l=0}^n \left[\begin{array}{c} \delta (k - 2 \cdot 3^l B) \\ + \delta (k + 2 \cdot 3^l B) + \delta (k) \end{array} \right] \right) \ast \hat{\epsilon}_B (k) \\ &= \left(\frac{\chi_{[-3^{n+1}B, 3^{n+1}B]} (k)}{3^{n+1} 2B} 2B \sum_{l=-\infty}^{\infty} \delta (k - 2Bl) \right) \ast \hat{\epsilon}_B (k) \end{aligned}$$

where

$$(B.20) \quad \hat{\epsilon}_B (k) = (2\pi)^{-1} \int \epsilon_B (x) e^{ikx} dx$$

is the inverse Fourier transform of $\epsilon_B (x)$ and $\ast_{l=0}^n f_l (k) = (f_0 \ast f_1 \ast \dots \ast f_n) (k)$ denotes a cascaded convolution operator. Taking the inverse Fourier transform, we obtain

$$(B.21) \quad \begin{aligned} \epsilon_{3^{n+1}B} (x) &= \left(\text{sinc} (3^{n+1} Bx) \ast \sum_{l=-\infty}^{\infty} \delta \left(x - \frac{2\pi l}{2B} \right) \right) \epsilon_B (x) \\ &= \sum_{l=-\infty}^{\infty} \text{sinc} \left(3^{n+1} B \left[x - \frac{\pi l}{B} \right] \right) \epsilon_B (x) \end{aligned}$$

which for $x = m\pi/B$ is

$$(B.22) \quad \begin{aligned} \epsilon_{3^{n+1}B} \left(\frac{m\pi}{B} \right) &= \sum_{l=-\infty}^{\infty} \text{sinc} (3^{n+1} \pi [m - l]) \epsilon_B \left(\frac{m\pi}{B} \right) \\ &= \sum_{l=-\infty}^{\infty} \delta_{ml} \epsilon_B \left(\frac{m\pi}{B} \right). \end{aligned}$$

By using the identity

$$(B.23) \quad \lim_{a \rightarrow \infty} 2a \text{sinc} (ax) = \delta (x)$$

Algorithm 1 Representation of $\text{sinc}(B_0x)$ as a sum of scaled cosinesGiven $0 \leq B_0 \in \mathbb{R}$

- (1) Compute $n = \log_3 \lfloor B_0 \rfloor + 1$
- (2) Set $B = B_0 3^{-n}$.
- (3) Solve the moment problem

$$h_n = B^{2n} (2n + 1)^{-1} = \sum_m \alpha_m (\omega_m^2)^n$$

for (α_m, ω_m) using the method of [29] (see Appendix A and Figure B.2)

- (4) Set $\theta_m = \omega_m B^{-1}$
- (5) Form the approximation (see Figure B.1)

$$\text{sinc}(B_0x) \approx \frac{1}{3^n} \sum_m \alpha_m \sum_{k=-(3^n-1)/2}^{(3^n-1)/2} \cos((\theta_m + 2k) Bx)$$

and the dominated convergence theorem (see page 14 of [9]), we have

$$\begin{aligned} \lim_{n \rightarrow \infty} 3^{n+1} 2B \epsilon_{3^{n+1}B}(x) &= \lim_{n \rightarrow \infty} \sum_{l=-\infty}^{\infty} 3^{n+1} 2B \text{sinc}\left(3^{n+1}B \left[x - \frac{\pi l}{B}\right]\right) \epsilon_B(x) \\ (B.24) \quad &= \sum_{l=-\infty}^{\infty} \delta\left(x - \frac{\pi l}{B}\right) \epsilon_B(x). \end{aligned}$$

□

The practical implications of Lemma 13 are as long as one has a good approximation $\text{sinc}(x) \approx \sum_m \alpha_m \cos(\theta_m x)$ over an interval around zero, the (α_m, θ_m) can be used to build up an approximation of (i) $\text{sinc}(Bx)$, for any $B \in \mathbb{R}$, on the same interval, (ii) $\text{sinc}(x)$ on any interval around zero or, equivalently, (iii) $\text{sinc}(Bx)$, for any $B \in \mathbb{R}$, on any interval around zero, as accurate as the initial approximation to $\text{sinc}(x)$. (see Figures B.1 and B.3) Algorithm 1 outlines our approach to approximating a sinc of arbitrary bandwidth as a sum of scaled cosines.

How about uniform sampling? Consider approximation of the integral

$$(B.25) \quad f(x) = \frac{1}{2B} \int_{-B}^B e^{ix\omega} d\omega = \text{sinc}(Bx)$$

by discretization of the integral using uniform sampling over the interval $[-B, B]$:

$$\begin{aligned} \tilde{f}_{B,N}(x) &= \frac{1}{2B} \frac{2B}{2N+1} \sum_{n=-N}^N e^{ix \frac{2B}{2N+1} n} \\ (B.26) \quad &= \frac{1}{2N+1} \frac{\sin(Bx)}{\sin\left(\frac{Bx}{2N+1}\right)} \end{aligned}$$

Because $\tilde{f}_{B,N}(x)$ is periodic with period $\pi B^{-1} (2N+1)$, it is also referred to as periodic sinc function.

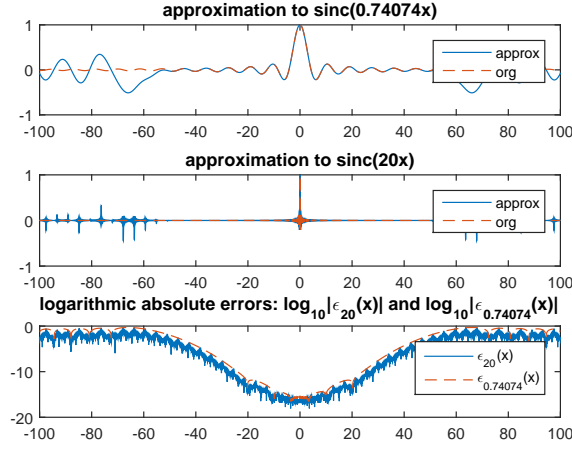


FIGURE B.1. Approximation of $\text{sinc}(Bx)$ by (B.2) using Algorithm 1. On top and middle plots, $\text{sinc}(Bx)$ and $\text{sinc}(B_0x)$ (red dashed) along with their approximations (solid blue), for $B = 3^{-3}20$ and $B_0 = 20$, respectively. On the bottom plot, the logarithmic absolute errors for B (red dashed) and B_0 (blue solid). As derived the error corresponding to B_0 is less than that of B .

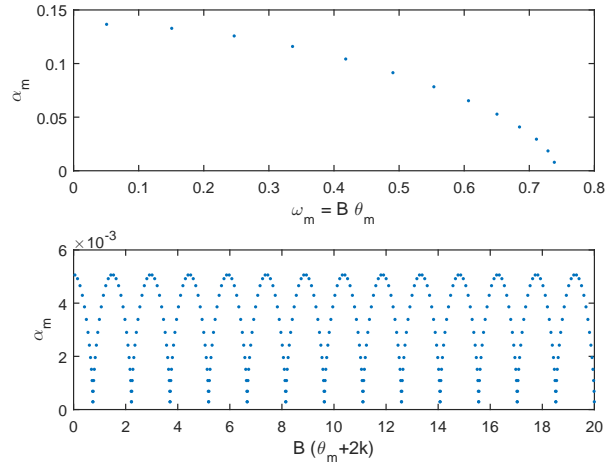


FIGURE B.2. On top plot, solution (α_m, ω_m) to the moment problem (B.3) for $B = 3^{-3}B_0$ and $B_0 = 20$ which is used to approximate $\text{sinc}(Bx)$ (see top plot in Figure B.1). On the bottom plot, $(\alpha_m, |\theta_m + 2k|B)_{k=-(3^3-1)/2}^{(3^3-1)/2}$ used to approximate $\text{sinc}(B_0x)$ (see middle plot in Figure B.1).

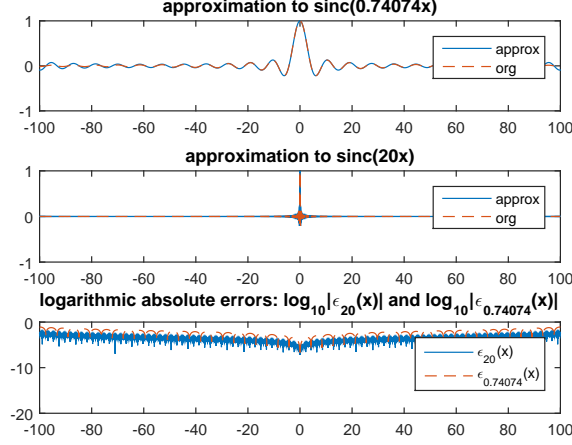


FIGURE B.3. Approximation of $\text{sinc}(Bx)$ by (B.26). On top and middle plots, $\text{sinc}(Bx)$ and $\text{sinc}(B_0x)$ (red dashed) along with their approximations $\tilde{f}_{B,N}(x)$ and $\tilde{f}_{B_0,N_0}(x)$ (solid blue) using uniform sampling, for $(B, N) = (3^{-3}20, 13)$ and $(B_0, N_0) = (20, 3^313)$, respectively. On the bottom plot, the logarithmic absolute errors for B (red dashed) and B_0 (blue solid). As derived the error corresponding to B_0 is less than that of B .

Using the Taylor series expansion of $(1-x)^{-1}$ and $\text{sinc}(x)$ around zero⁵ series representation of the error becomes

$$\begin{aligned}
 \epsilon_B(x) &= f(x) - \tilde{f}_{B,N}(x) \\
 &= \frac{\sin(Bx)}{Bx} \left(1 - \frac{1}{1 - \left[1 - \text{sinc}\left(\frac{Bx}{2N+1}\right) \right]} \right) \\
 \text{(B.27)} \quad &= \text{sinc}(Bx) \sum_{m=1}^{\infty} (-1)^{m+1} \left[\sum_{n=1}^{\infty} \frac{(-1)^n}{(2n+1)!} \left(\frac{B}{2N+1} x \right)^{2n} \right]^m
 \end{aligned}$$

which decays like $\mathcal{O}\left((2N+1)^{-2}\right)$ within the vicinity of zero and increases away from zero for $|x| < \pi(2B)^{-1}(2N+1)$. Consequently, maximum absolute error is obtained at $|x| = \pi(2B)^{-1}(2N+1)$ which is

$$\begin{aligned}
 \left| \epsilon_B \left(\frac{(2N+1)\pi}{2B} \right) \right| &= \left| \text{sinc} \left(\frac{(2N+1)\pi}{2} \right) \left(1 - \text{sinc} \left(\frac{\pi}{2} \right)^{-1} \right) \right| \\
 \text{(B.28)} \quad &= \frac{2}{(2N+1)\pi} \left(\frac{\pi}{2} - 1 \right)
 \end{aligned}$$

and decays in the order of N . For $(N, B) = (13, 20 \times 3^{-3})$ and $(N_0, B_0) = (13 \times 3^3, 20)$ we present $\tilde{f}_{B,N}(x)$ and $\tilde{f}_{B_0,N_0}(x)$ in Figure B.3.

⁵, $(1-x)^{-1} = \sum_{m=0}^{\infty} x^m$ and $\text{sinc}(x) = \sum_{n=0}^{\infty} \frac{(-1)^n}{(2n+1)!} x^{2n}$

Lemma 13 can be generalized to any arbitrary function:

Theorem 15. *Let*

$$(B.29) \quad \epsilon_B(x) = \text{sinc}(Bx) - f(x).$$

Then

$$(B.30) \quad \left| \text{sinc}(3^n Bx) - \frac{1}{3^n} \left[\sum_{l=1}^{(3^n-1)/2} 2 \cos(2Blx) + 1 \right] f(x) \right| \leq |\epsilon_B(x)|, \text{ for } n \geq 0.$$

Proof. The proof follows from arguments that are similar to those in Lemma 13. \square

Corollary 16. *Let*

$$(B.31) \quad \epsilon_B(x) = \text{sinc}(Bx) - \sum_m \alpha_m \exp(-\gamma_m x^2),$$

such that $\text{Re}\{\gamma_m\} > 0$. *Then*

$$(B.32) \quad \left| \text{sinc}(3^n Bx) - \frac{1}{3^n} \sum_m \sum_{l=-(3^n-1)/2}^{(3^n-1)/2} a_{m,l} g_{m,l}(x) \right| \leq |\epsilon_B(x)|, \text{ for } n \geq 0.$$

where $a_{m,l} = \alpha_m \exp\left(i \frac{(Bl)^2}{\text{Im}\{\gamma_m\}}\right)$ and

$$(B.33) \quad \begin{aligned} g_{m,l}(x) &= \exp(-\text{Re}\{\gamma_m\} x^2) \\ &\times \exp\left(-i \text{Im}\{\gamma_m\} \left(x - \frac{Bl}{\text{Im}\{\gamma_m\}}\right)^2\right). \end{aligned}$$

Proof. This is a direct consequence of Theorem 15 and identities

$$(B.34) \quad \left[\sum_{l=1}^{(3^n-1)/2} 2 \cos(2Blx) + 1 \right] \exp(-\gamma_m x^2) = \sum_{l=-(3^{n+1}-1)/2}^{(3^{n+1}-1)/2} \exp(-\gamma_m x^2 + i2Blx)$$

$$(B.35) \quad \begin{aligned} &\exp(-\gamma_m x^2 + i2Blx) \\ &= \exp(-\text{Re}\{\gamma_m\} x^2) \exp\left(-i \text{Im}\{\gamma_m\} \left(x - \frac{Bl}{\text{Im}\{\gamma_m\}}\right)^2\right) \exp\left(i \frac{(Bl)^2}{\text{Im}\{\gamma_m\}}\right) \end{aligned}$$

\square

Corollary 16 says that the sinc function can be approximated as a sum of shifted, Gaussian tapered chirps. One can determine (α_m, γ_m) using the method in Appendix A by solving the appropriate moment problem (see Step 3 of Algorithm 2). This type of approximations of $\text{sinc}(x)$ can be used to construct a multiresolution scheme for band-limited function as an alternative to existing multiscale approaches. It is important to point out that unlike chirplet decomposition methods presented in [19, 3], the moment problem provides an explicit solution for (α_m, γ_m) while coupling the real and imaginary part of the complex Gaussian parameters γ_m . Algorithm 2 outlines approximating a sinc of arbitrary bandwidth as a sum of scaled cosines based on the moment problem and Corollary 16. A corresponding example is presented in Figure B.4.

Algorithm 2 Representation of $\text{sinc}(B_0x)$ as a sum of chirplets

Given $0 \leq B_0 \in \mathbb{R}$

- (1) Compute $n = \log_3 \lfloor B_0 \rfloor + 1$
- (2) Set $B = B_0 3^{-n}$.
- (3) Solve the moment problem

$$h_n = B^{2n} \frac{n!}{(2n+1)!} = \sum_m \alpha_m \gamma_m^n$$

for (α_m, γ_m) using the method of [29] (see Appendix A)

- (4) Form the approximation

$$\text{sinc}(B_0x) \approx \frac{1}{3^n} \sum_m \sum_{l=-(3^n-1)/2}^{(3^n-1)/2} \alpha_m \left[\begin{array}{l} \exp\left(i \frac{(Bl)^2}{\text{Im}\{\gamma_m\}}\right) \exp(-\text{Re}\{\gamma_m\} x^2) \\ \times \exp\left(-i \text{Im}\{\gamma_m\} \left(x - \frac{Bl}{\text{Im}\{\gamma_m\}}\right)^2\right) \end{array} \right]$$

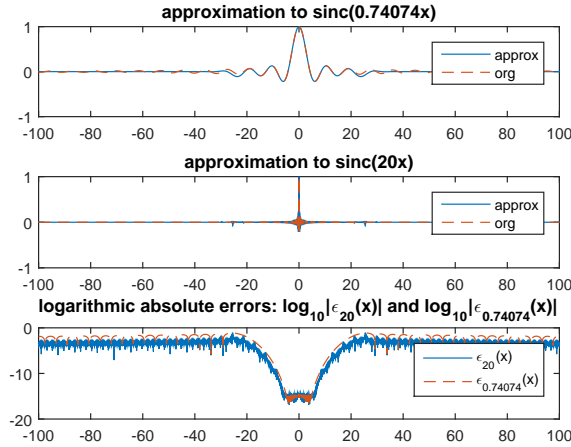


FIGURE B.4. Approximation of $\text{sinc}(Bx)$ as a sum of chirplets (see Corollary 16) using Algorithm 2. On top and middle plots, $\text{sinc}(Bx)$ and $\text{sinc}(B_0x)$ (red dashed) along with their approximations (solid blue), for $B = 3^{-3}20$ and $B_0 = 20$, respectively. On the bottom plot, the logarithmic absolute errors for B (red dashed) and B_0 (blue solid). As derived the error corresponding to B_0 is less than that of B .

APPENDIX C. T -LIMITED FUNCTIONS

In this section we consider triangle and tetrahedral limited functions both of whom are referred to as T -limited functions. The distinction of two class of T -limited function should be clear from the dimensions of their variables.

C.1. Triangle-limited functions. We say a function $f(x, y)$, $(x, y) \in \mathbb{R}^2$ is triangle limited if its Fourier transform $\hat{f}(k_x, k_y)$ is supported within a triangular region

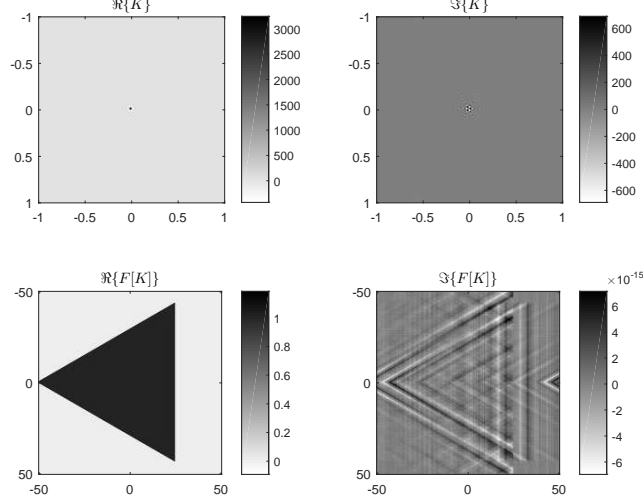


FIGURE C.1. Real, imaginary parts of $K(x, y) = K_{\Delta}(x, y) \exp(-i2\pi\Delta p \frac{2}{3}x)$ and its Fourier transform for $\Delta p = 75$ and $s = \sqrt{3}^{-1}$. The horizontal axis are x and k_x axis and the vertical axis are y and k_y , appropriately.

$T \subset \mathbb{R}^2$. Without loss of generality let $T \subset \mathbb{R}^2$ be parametrize by

$$(C.1) \quad T = \{(k_x, k_y) \mid 0 \leq k_x \leq \Delta p, |k_y| \leq k_x s, \}$$

for some $\Delta p, s \in \mathbb{R}^+$. Define $K_{\Delta}(x, y)$ to be

$$(C.2) \quad \begin{aligned} K_{\Delta}(x, y) &= \int_0^{\Delta p} \int_{-k_x s}^{k_x s} e^{i2\pi(k_x x + k_y y)} dk_y dk_x \\ &= \frac{\Delta p}{2\pi y} \left[\text{cosinc}(2\pi\Delta p(x + sy)) - \text{cosinc}(2\pi\Delta p(x - sy)) \right] \\ &\quad \left[-i \left[\text{sinc}(2\pi\Delta p(x + sy)) - \text{sinc}(2\pi\Delta p(x - sy)) \right] \right] \end{aligned}$$

We refer to K_{Δ} as the kernel for T -limited functions. Let us consider the kernel

$$K(x, y) = K_{\Delta}(x, y) \exp\left(-i2\pi\Delta p \frac{2}{3}x\right)$$

for $s = \sqrt{3}^{-1}$. Fourier transform of $K(x, y)$ is the characteristic function over an equilateral triangle whose center of mass is at the origin. For $\Delta p = 75$, we present the kernel $K(x, y)$ and its Fourier transform in Figure C.1. Next we will give two ways to construct quadratures for discrete Fourier approximation of $K_{\Delta}(x, y)$ which can be generalized to construct quadratures for simplexes in higher dimensions, too.

Proposition 17. $K_{\Delta}(x, y)$ satisfies the following scaling property

$$(C.3) \quad K_{\Delta}(x, y) = \frac{1}{4} \left[\begin{aligned} &K_{\Delta}\left(\frac{x}{2}, \frac{y}{2}\right) (1 + 2e^{i\pi\Delta p x} \cos(\pi\Delta p s y)) \\ &+ e^{i2\pi\Delta p x} K_{\Delta}\left(-\frac{x}{2}, \frac{y}{2}\right) \end{aligned} \right]$$

Consequently, let $K_{\Delta, m}(x, y) = K_{\Delta}(2^m x, 2^m y)$. Then

$$(C.4) \quad K_{\Delta, m}(x, y) = \frac{1}{4} \left[\begin{aligned} &K_{\Delta, m-1}(x, y) (1 + 2e^{i\pi 2^m \Delta p x} \cos(\pi 2^m \Delta p s y)) \\ &+ e^{i\pi 2^{m+1} \Delta p x} K_{\Delta, m-1}(-x, y) \end{aligned} \right]$$

Proof. This is a direct consequence self similarity of isosceles triangle which is used to decompose integral representation of $K_\Delta(x, y)$ using the identity

$$(C.5) \quad \int_0^{\Delta p} \int_{-k_x s}^{k_x s} dk_y dk_x = \left[\begin{array}{l} \int_0^{\Delta p/2} \int_{-k_x s}^{k_x s} + \int_{\Delta p/2}^{\Delta p} \int_{-(\Delta p - k_x)s}^{(\Delta p - k_x)s} \\ + \int_{\Delta p/2}^{\Delta p} \int_{(\Delta p - k_x)s}^{k_x s} + \int_{\Delta p/2}^{\Delta p} \int_{-k_x s}^{(k_x - \Delta p)s} \end{array} \right] dk_y dk_x$$

$$\text{and } \frac{1}{4} K_\Delta\left(\frac{x}{2}, \frac{y}{2}\right) = \int_0^{\Delta p/2} \int_{-k_x s}^{k_x s} e^{i2\pi(k_x x + k_y y)} dk_y dk_x \quad \square$$

Corollary 18. Let $K_{\Delta, m}(x, y) = K_\Delta(2^m x, 2^m y)$. Then

$$(C.6) \quad K_{\Delta, m-1}(x, y) = \left[\frac{\left(\begin{array}{l} K_{\Delta, m}(x, y) (1 + 2e^{-i\pi 2^m \Delta p x} \cos(\pi 2^m \Delta p s y)) \\ - e^{i\pi 2^{m+1} \Delta p x} K_{\Delta, m}(-x, y) \end{array} \right)}{\cos^2(\pi 2^m \Delta p s y) + \cos(\pi 2^m \Delta p x) \cos(\pi 2^m \Delta p s y)} \right]$$

Proof. Considering $K_{\Delta, m}(x, y)$ and $K_{\Delta, m}(-x, y)$, computation of

$$(C.7) \quad \frac{K_{\Delta, m}(x, y)}{e^{i\pi 2^{m+1} \Delta p x}} - \frac{K_{\Delta, m}(-x, y)}{(1 + 2e^{-i\pi 2^m \Delta p x} \cos(\pi 2^m \Delta p s y))} = \frac{1}{4} \left[\begin{array}{l} K_{\Delta, m-1}(x, y) \\ \times \left[\frac{|1 + 2e^{i\pi 2^m \Delta p x} \cos(\pi 2^m \Delta p s y)|^2 - 1}{e^{i\pi 2^{m+1} \Delta p x} (1 + 2e^{-i\pi 2^m \Delta p x} \cos(\pi 2^m \Delta p s y))} \right] \end{array} \right]$$

leads to (C.6). □

C.1.1. *Discrete Fourier approximation of $K_\Delta(x, y)$.* For a discrete representation of the kernel let us consider a bounded region $(x, y) \in S$. T -limited projection operator P_Δ and T -limited projection f_Δ of f restricted to the region S are defined by

$$(C.8) \quad \begin{aligned} P_\Delta[f](x, y) &= f_\Delta(x, y) \\ &= \int_S f(x', y') K_\Delta(x - x', y - y') dx' dy' \end{aligned}$$

Noticing that argument of K_Δ ranges over

$$(C.9) \quad S + S = \left\{ (x, y) \mid (x, y) = (x_1, y_1) + (x_2, y_2), (x_n, y_n)_{n=1,2} \in S \right\},$$

in order to compute $f_\Delta(x, y)$ accurately over the region S , one should have an accurate representation of K_Δ inside $S + S$.

Recalling (C.2),

$$\begin{aligned}
(C.10) \quad K_{\Delta}(x, y) &= \int_0^{\Delta p} \int_{-k_x s}^{k_x s} e^{i2\pi(k_x x + k_y y)} dk_y dk_x \\
&= \frac{\Delta p}{2\pi i} s \int_{-1}^1 \partial_x \left[\int_0^1 e^{i2\pi \Delta p (x + s k_y y) k_x} dk_x \right] dk_y \\
&\approx \frac{\Delta p}{2\pi i} s \int_{-1}^1 \partial_x \left[\sum_{m=1}^M \alpha_m e^{i2\pi \Delta p (x + s k_y y) k_x [m]} \right] dk_y
\end{aligned}$$

$$\begin{aligned}
(C.11) \quad &= \Delta p^2 s \sum_{m=1}^M \left(\alpha_m k_x [m] e^{i2\pi \Delta p x k_x [m]} \right. \\
&\quad \left. \times \left[\int_{-1}^1 e^{i2\pi \Delta p s k_x [m] y k_y} dk_y \right] \right) \\
&\approx 2\Delta p^2 s \sum_{m=1}^M \left(\alpha_m k_x [m] e^{i2\pi \Delta p x k_x [m]} e^{-i2\pi 2\Delta p s k_x [m] y} \right. \\
&\quad \left. \times \left[\sum_{n=1}^{N(m)} \beta_{m,n} e^{i2\pi \Delta p s k_x [m] y 2k_y [m,n]} \right] \right)
\end{aligned}$$

where $(\alpha_m, k_x [m])$ and $(\beta_{m,n}, k_y [m, n])$ are quadratures for approximating sinc as a sum of cosines (See (B.2) and consider B equal to $2\pi \Delta p (X + sY)$ and $4\pi \Delta p s k_x [m] Y$, respectively, where $X = \max_{(x,y) \in S+S} |x|$ and $Y = \max_{(x,y) \in S+S} |y|$.) for a desired accuracy, which determines the accuracy of approximating K_{Δ} inside $S + S$.

Corollary 19. *Let $\tilde{K}_{\Delta, m}(x, y)$ be an approximation of $K_{\Delta, m}(x, y)$ and $\epsilon_{\Delta, m}(x, y) = K_{\Delta, m}(x, y) - \tilde{K}_{\Delta, m}(x, y)$ be the associated error. Then*

$$(C.12) \quad |\epsilon_{\Delta, m}(x, y)| \leq \frac{1}{4} [3|\epsilon_{\Delta, m-n}(x, y)| + |\epsilon_{\Delta, m-n}(-x, y)|].$$

Furthermore, if $|\epsilon_{\Delta, m_0}(x, y)| = |\epsilon_{\Delta, m_0}(-x, y)|$ for an $m_0 \in \mathbb{Z}$, then $|\epsilon_{\Delta, m}(x, y)| \leq |\epsilon_{\Delta, m_0}(x, y)|$ for all $m \geq m_0$. Consequently,

$$\begin{aligned}
(C.13) \quad \left| K_{\Delta}(x, y) - \tilde{K}_{\Delta, m}(2^{-m}x, 2^{-m}y) \right| &= |\epsilon_{\Delta, m}(2^{-m}x, 2^{-m}y)| \\
&\leq |\epsilon_{\Delta}(2^{-m}x, 2^{-m}y)|
\end{aligned}$$

Proof. Proof by induction using the identity

$$(C.14) \quad \epsilon_{\Delta, m}(x, y) = \frac{1}{4} \left[\epsilon_{\Delta, m-1}(x, y) (1 + 2e^{i2\pi \Delta p x} \cos(2\pi \Delta p s y)) \right. \\ \left. + e^{i4\pi \Delta p x} \epsilon_{\Delta, m-1}(-x, y) \right]$$

obtained from (C.4). □

Corollary 19 says that for approximating $K_{\Delta, m}(x, y)$ with a desired error bound ϵ over a desired region centered around zero, it is sufficient to find an approximation to $K_{\Delta, m_0}(x, y)$ for any integer (including negative integers) $m_0 < m$ whose error is less than or equal to ϵ within the vicinity of zero. We present $\tilde{K}_{\Delta, m}(2^{-m}x, 2^{-m}y)$ and $|\epsilon_{\Delta, m}(2^{-m}x, 2^{-m}y)|$ for $m_0 = 0$ and $m = 0, 1, \dots, 7$ in Figures C.4 and C.5.

C.1.2. Nodes capturing rotational invariance of equilateral triangle. Let us consider the equilateral triangle T_E with each side equal to 1 and center of mass at the origin. T_E is equivalent to the triangle T of (C.1) with $\Delta p = \sqrt{3}/2$ and $s = \sqrt{3}^{-1}$. While we can construct discrete Fourier approximation of the kernel for the equilateral triangle using the method in Appendix C.1.1, constructed nodes $(k_x [m], k_y [m, n])$ do not necessarily satisfy the rotational invariance of equilateral triangle (see Figure C.2).

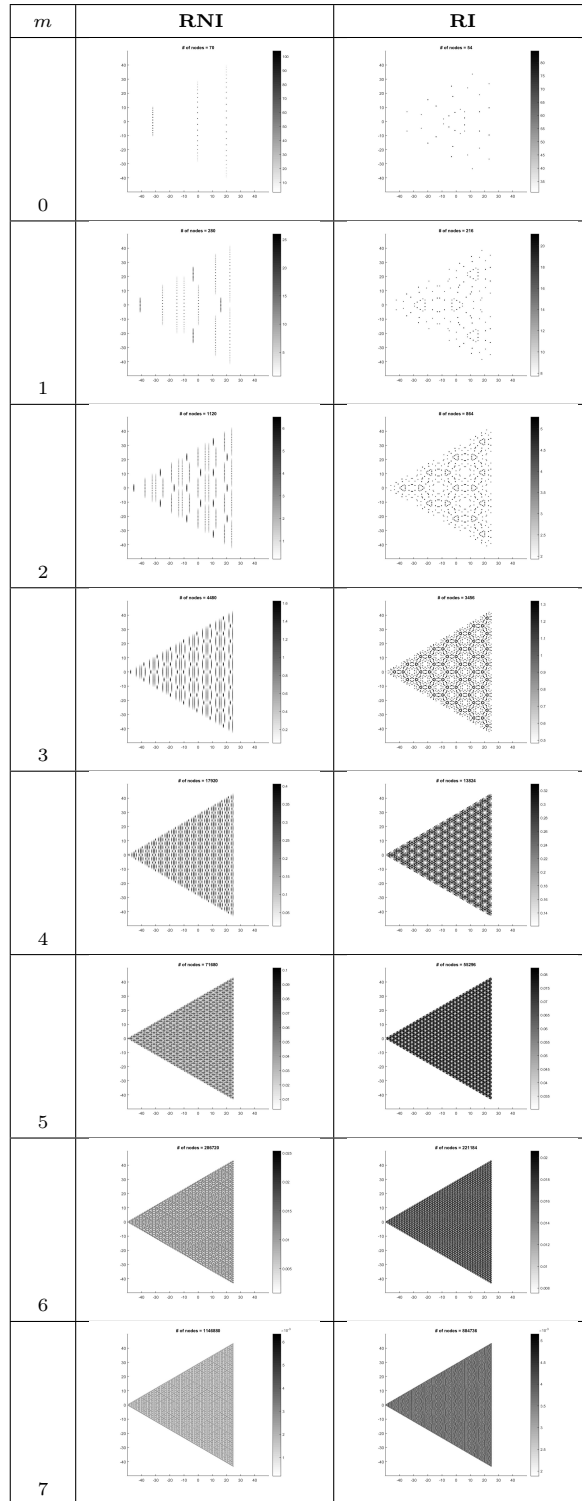


FIGURE C.2. Rotationally not invariant (RNI column) and rotationally invariant (RI column) Fourier quadratures for $K_{\Delta}(x, y)$. The horizontal axis is k_x and the vertical axis is k_y .

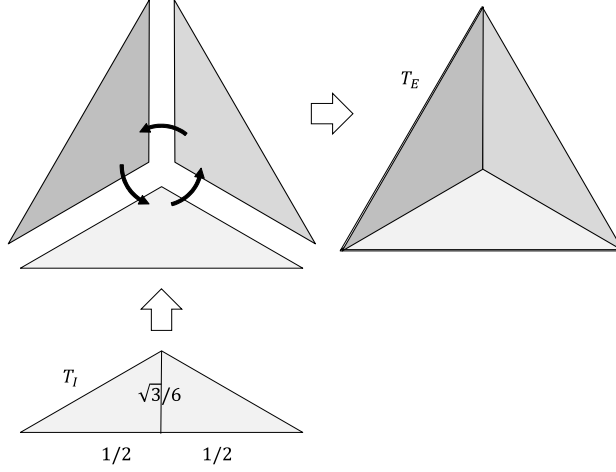


FIGURE C.3. Construction of nodes that satisfy the rotational invariance of equilateral triangle can be achieved by first constructing nodes for the lightest gray triangle followed by rotating and accumulating the constructed nodes.

In order to preserve the rotational invariance of the equilateral triangle among the nodes, one can construct nodes for the isosceles triangle T_I which is triangle T of (C.1) with $\Delta p = \sqrt{3}/6$ and $s = \sqrt{3}^{-1}$, then rotate these nodes by $2\pi/3$ and $4\pi/3$ to construct nodes satisfying the rotational invariance of the equilateral triangle (see Figure C.2) as illustrated in Figure C.3. Our observation is, for the same or less number of nodes, the nodes with rotational symmetry provide a more accurate discretization of the Fourier approximation of the kernel $K_\Delta(x, y)$ compared to nodes without rotational symmetry (see Figures C.4 and C.5).

C.2. Tetrahedron limited functions. We say a function $f(x, y, z)$, $(x, y, z) \in \mathbb{R}^3$ is tetrahedron limited if its Fourier transform $\hat{f}(k_x, k_y, k_z)$ is supported within a tetrahedral region $T \subset \mathbb{R}^3$:

$$(C.15) \quad f(x, y) = \int_T \hat{f}(k_x, k_y, k_z) e^{2\pi i(k_x x + k_y y + k_z z)} dk_z dk_y dk_x$$

Without loss of generality, let T be parametrized by

$$(C.16) \quad T = \{(k_x, k_y, k_z) \mid 0 \leq k_z \leq h, 0 \leq k_y \leq \Delta p k_z, |k_x| \leq k_y s, \}$$

for some $\Delta p, s, h \in \mathbb{R}^+$. Define $K_\triangleleft(x, y, z)$ to be

$$(C.17) \quad \begin{aligned} & K_\triangleleft(x, y, z) \\ &= \int_0^h \int_0^{k_z \Delta p} \int_{-k_y s}^{k_y s} e^{i2\pi(k_x x + k_y y + k_z z)} dk_x dk_y dk_z \\ &= -\frac{h^2 \Delta p}{2\pi x} \left\{ \frac{\text{expc}(i2\pi h[z + \Delta p(y + sx)]) - \text{expc}(i2\pi h z)}{2\pi h \Delta p(y + sx)} \right. \\ & \quad \left. - \frac{\text{expc}(i2\pi h[z + \Delta p(y - sx)]) - \text{expc}(i2\pi h z)}{2\pi h \Delta p(y - sx)} \right\} \end{aligned}$$

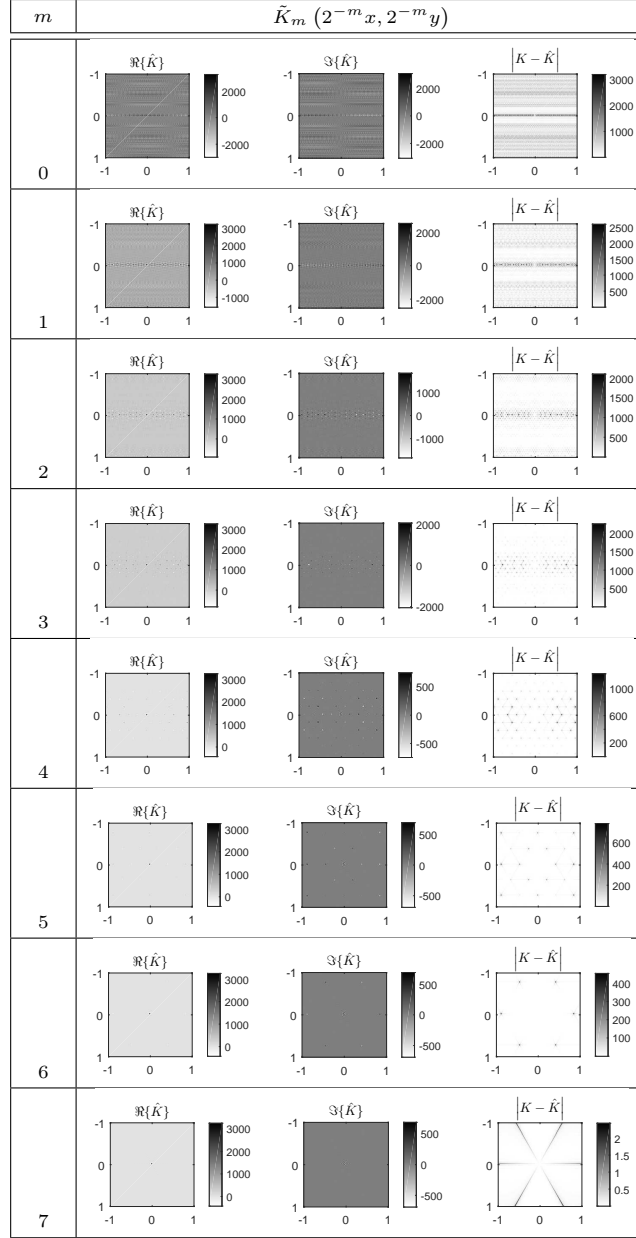


FIGURE C.4. Approximation of the kernel $K_\Delta(x, y)$ by $\tilde{K}_{\Delta, m}(2^{-m}x, 2^{-m}y)$ using the RNI quadratures in Figure C.2. The horizontal axis is x and the vertical axis is y .

where $\text{expc}(x) = (\exp(x) - 1)x^{-1}$, implying $\text{expc}(ix) = \text{sinc}(x) + i\text{cosinc}(x)$, with $\text{cosinc}(x) = (1 - \cos(x))x^{-1}$. For an equilateral tetrahedron, choose $h = \sqrt{\frac{2}{3}}$,

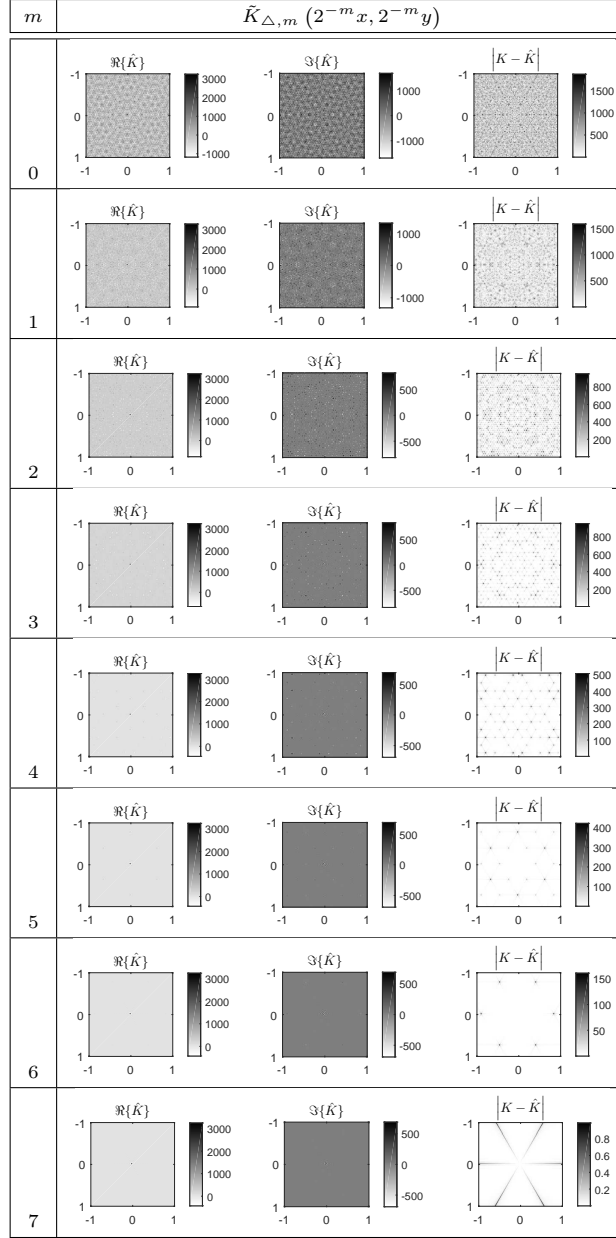


FIGURE C.5. Approximation of the kernel $K_{\Delta}(x, y)$ by $\tilde{K}_{\Delta,m}(2^{-m}x, 2^{-m}y)$ using the RI quadratures in Figure C.2. The horizontal axis is x and the vertical axis is y .

$\Delta p = \frac{\sqrt{3}}{6}h$, $s = \sqrt{3}$ and add the resulting kernel with its $\frac{2}{3}\pi$ and $\frac{4}{3}\pi$ rotated versions around the z -axis (see Figure C.6).

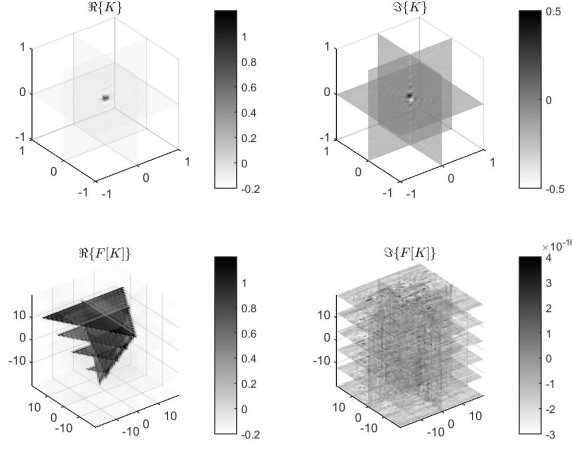


FIGURE C.6. Real, imaginary parts of $K(x, y, z) = B^{-3} \sum_{n=0}^2 K_{\triangleleft}(Bx_n, By_n, Bz_n) \exp\left(i2\pi B \left[-\frac{1}{2}z + \left(\frac{1}{2} + \frac{\sqrt{3}}{3}y\right)\right]\right)$ and its Fourier transform for $h = \sqrt{\frac{2}{3}}$, $\Delta p = \frac{\sqrt{3}}{6}h$, $s = \sqrt{3}$ and $B = 20$. Here $[x_n, y_n, z_n]^T = R_{[0,0,1]} \left(\frac{2}{3}\pi n\right) [x, y, z]^T$ for $n = 0, 1, 2$.

Similar to the triangle-limited case, construction of the nodes is equivalent to discretization of the Fourier integral using cascaded Gauss-Legendre quadratures that can accurately approximate the representation kernel within a region of interest:

$$\begin{aligned}
 & K_{\triangleleft}(x, y, z) \\
 &= \int_0^h \int_0^{k_z \Delta p} \int_{-k_y s}^{k_y s} e^{i2\pi(k_x x + k_y y + k_z z)} dk_x dk_y dk_z \\
 &= -\frac{h \Delta p s}{4\pi^2} \partial_y \partial_z \int_{-1}^1 \int_0^1 \int_0^1 e^{i2\pi h(\Delta p[s k_x x + y] k_y + z) k_z} dk_z dk_y dk_x \\
 \text{(C.18)} \quad &= 2h^3 \Delta p^2 s \sum_{m,n,l} \left\{ \alpha_m \beta_{m,n} \gamma_{m,n,l} k_z^2 [m] k_y [m, n] \right. \\
 & \quad \left. \times e^{i2\pi h(\Delta p[s(2k_x [m,n,l]-1)x + y] k_y [m,n] + z) k_z [m]} \right\}
 \end{aligned}$$

where $(\alpha_m, k_z [m])$, $(\beta_{m,n}, k_y [m, n])$ and $(\gamma_{m,n,l}, k_x [m, n, l])$ are quadratures for approximating $\text{sinc}(Bx)$ as a sum of cosines (see (B.2)) for B equal to $2\pi h(\Delta p(Y + sX) + Z)$ and $2\pi h \Delta p k_z [m](Y + sX)$ and $4\pi h \Delta p s k_z [m] k_y [m, n] X$, respectively, where $X = \max_{(x,y,z) \in S+S} |x|$, $Y = \max_{(x,y,z) \in S+S} |y|$ and $Z = \max_{(x,y,z) \in S+S} |z|$.

Let us consider a unit tetrahedron, i.e. a tetrahedron with all sides equal to one. In order to construct nodes that satisfy the symmetries of the unit tetrahedron, first construct nodes for the sub-tetrahedron with $s = \sqrt{3}$, $\Delta p = \sqrt{2}$, $h = \sqrt{24}^{-1}$ (see Figure C.7) and then use the symmetry group of the regular tetrahedron. Namely, apply rotations $R_{\hat{v}_4} \left(\frac{2}{3}\pi n\right) R_{\hat{v}_1} \left(\frac{2}{3}\pi m\right)$, for $n, m = 0, 1, 2$, and $R_{\hat{v}_4} \left(\frac{2}{3}\pi n\right) R_{\hat{v}_2} \left(\frac{4}{3}\pi\right)$ to the quadrature of sub-tetrahedron. Here $\hat{v} = v/|v|$ is the unit vector pointing

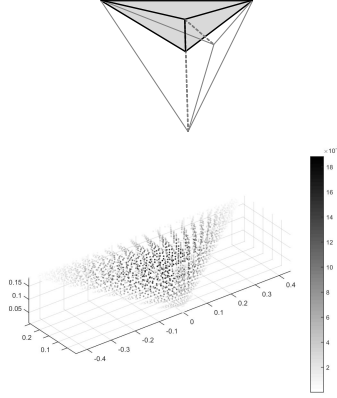


FIGURE C.7. Construction of the nodes that satisfies the isometries of the tetrahedron can be obtained by construct nodes for the shaded tetrahedron (top) and apply symmetry group of the tetrahedon (see Figure C.8) to the constructed nodes (bottom).

along vector v with v_i , for $i = 1, 2, 3, 4$, given by

$$(C.19) \quad v_1 = \left[-\frac{1}{2}, -\frac{\sqrt{3}}{6}, -\frac{1}{6}\sqrt{\frac{3}{2}} \right]$$

$$(C.20) \quad v_2 = \left[\frac{1}{2}, -\frac{\sqrt{3}}{6}, -\frac{1}{6}\sqrt{\frac{3}{2}} \right]$$

$$(C.21) \quad v_3 = \left[0, \frac{\sqrt{3}}{3}, -\frac{1}{6}\sqrt{\frac{3}{2}} \right]$$

$$(C.22) \quad v_4 = \left[0, 0, \sqrt{\frac{2}{3}} - \frac{1}{6}\sqrt{\frac{3}{2}} \right].$$

and

$$(C.23) \quad R_u(\theta) = \begin{bmatrix} r_1(\theta) & r_{123}(-\theta) & r_{123}(\theta) \\ r_{123}(\theta) & r_2(\theta) & r_{231}(-\theta) \\ r_{132}(-\theta) & r_{231}(\theta) & r_3(\theta) \end{bmatrix}$$

is the matrix for a rotation by an angle θ around the unit vector $u = [u_1, u_2, u_3]$ with

$$(C.24) \quad r_i(\theta) = \cos \theta + u_i^2 (1 - \cos \theta)$$

$$(C.25) \quad r_{ijk}(\theta) = u_i u_j (1 - \cos \theta) + u_k \sin \theta.$$

The quadrature generated for the regular tetrahedron using the discussed steps is presented in Figure C.8 .

APPENDIX D. CONE-LIMITED FUNCTIONS

In seismic or electromagnetic signal processing the signal is modeled through the wave equation. For an acoustic homogeneous medium with wave speed $c = p^{-1}$,

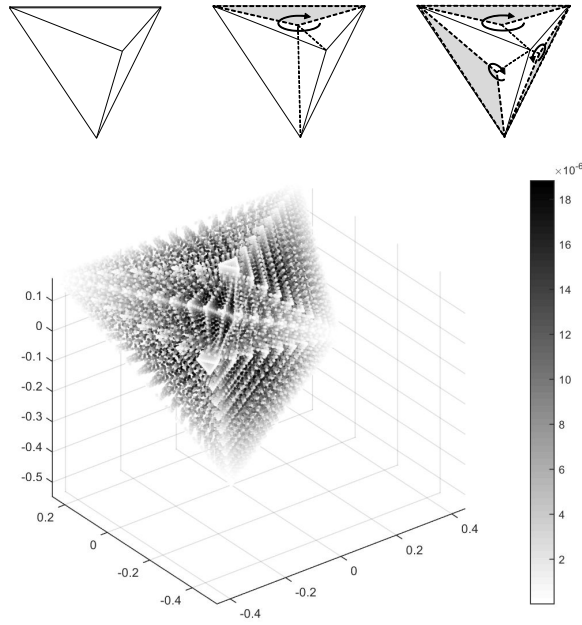


FIGURE C.8. A regular tetrahedron (top left) is symmetric under rotation with respect to one of its faces (top middle). Its rotational symmetries with respect to 3 out of 4 faces (top right). There are a total of $4 \times 3 \times 2 = 24$ isometries of the tetrahedron which form the symmetry group of the tetrahedron. Out of these 12 of them preserves orientation which are used to generate the corresponding quadrature (bottom) from the quadrature of the sub-tetrahedron in Figure C.7.

the wave equation provides a dispersion relationship between the frequency ω and wave number \mathbf{k} , $|\mathbf{k}| = \omega p$. For a heterogeneous medium, the dispersion relationship becomes an inequality $|\mathbf{k}| \leq \omega p_{\max}$ where the maximum slowness $p_{\max} = c_{\min}^{-1}$ is the one over the minimum speed c_{\min} of the heterogeneous medium. Given the maximum frequency ω_0 of the recording system, the Fourier transform of the measurement is supported inside the cone $C = \{(\omega, \mathbf{k}) \in \mathbb{R} \times \mathbb{R}^n | \omega \in [-\omega_0, \omega_0], |\mathbf{k}| \leq \omega p_{\max}\}$ for $t \in \mathbb{R}$ and $\mathbf{x} \in \mathbb{R}^n$, which is referred to as the signal cone. Temporal and spatial Fourier transform of video images also have their Fourier transforms supported effectively in a similar cone.

We say a function $f(t, \mathbf{x})$ is cone-limited, C -limited for short, if its Fourier transform $\hat{f}(\omega, \mathbf{k})$ is supported within the cone C . C -limited functions are invariant under convolution with the kernel $K(t, \mathbf{x})$, whose Fourier transform, $\hat{K}(\omega, \mathbf{k})$, is equal to one within C :

$$(D.1) \quad K(t, \mathbf{x}) = \int_C e^{i2\pi(\omega t - \mathbf{k} \cdot \mathbf{x})} d\omega d\mathbf{k}.$$

For n odd, $K(t, \mathbf{x})$ can be represented in terms of elementary functions. For example, for $n = 1$ and $n = 3$, we have

$$(D.2) \quad K(t, x) = \frac{\omega_0}{\pi x} \begin{pmatrix} \text{cosinc}(2\pi\omega_0 [t + p_{\max}x]) \\ -\text{cosinc}(2\pi\omega_0 [t - p_{\max}x]) \end{pmatrix}$$

and

$$(D.3) \quad K(t, \mathbf{x}) = -\frac{\omega_0}{\pi r} \partial_r \left\{ \frac{1}{r} \begin{bmatrix} \text{cosinc}(2\pi\omega_0 [t + p_{\max}r]) \\ -\text{cosinc}(2\pi\omega_0 [t - p_{\max}r]) \end{bmatrix} \right\},$$

respectively. On the other hand, for n even, $K(t, \mathbf{x})$ is a multivariate special function. For example, for $n = 2$, we have

$$(D.4) \quad \begin{aligned} K(t, \mathbf{x}) &= \int_0^{2\pi} \int_0^{p_{\max}} \int_{-\omega_0}^{\omega_0} e^{i2\pi\omega(t-pr\cos\theta)} \omega^2 p \, d\omega \, dp \, d\theta \\ &= \frac{2\omega_0^2 p_{\max}}{\pi r} \int_0^1 J_1(2\pi\omega r \omega_0 p_{\max}) \cos(2\pi\omega\omega_0 t) \omega \, d\omega \end{aligned}$$

where $|\mathbf{x}| = r$ and $J_n(t)$ is the n^{th} order Bessel function of the first kind. Because all the cases for n even, requires evaluation of an integral of the form (D.4), for the ease of our discussion we will focus on the case $n = 2$.

Following [29], $J_1(x)$ can be approximate by $J_1(x) \approx \sum_{m=1}^M \alpha_m \text{cosinc}(\gamma_m x)$, where (α_m, γ_m) satisfies a moment problem. (see Table 1 in Appendix A). Consequently, we have

$$(D.5) \quad \begin{aligned} K(t, \mathbf{x}) &\approx \tilde{K}(t, \mathbf{x}) \\ &= \frac{\omega_0}{\pi^2} \sum_{m=1}^M \frac{\alpha_m}{\gamma_m} \begin{pmatrix} \text{sinc}(2\pi\omega_0 t) \\ -\frac{1}{2} \begin{bmatrix} \text{sinc}(2\pi\omega_0 [\gamma_m p_{\max} r - t]) \\ +\text{sinc}(2\pi\omega_0 [\gamma_m p_{\max} r + t]) \end{bmatrix} \end{pmatrix} \end{aligned}$$

The least square error is given by

$$(D.6) \quad \int \left| K(t, \mathbf{x}) - \tilde{K}(t, \mathbf{x}) \right|^2 dt \, d\mathbf{x} = \frac{4\omega_0^3 p_{\max}^2}{\pi^2 3} \left(\frac{1}{2} - \sum_{m=1}^M \alpha_m \gamma_m + \sum_{m, m'=1}^M \alpha_m w_{m, m'} \alpha_{m'} \right),$$

where

$$(D.7) \quad w_{m, m'} = \int_{\mathbb{R}^+} \frac{\sin^2(\gamma_m r/2)}{\gamma_m r/2} \frac{\sin^2(\gamma_{m'} r/2)}{\gamma_{m'} r/2} \frac{dr}{r},$$

which can be explicitly computed using integration by parts and the identities 3.827-3.828 on pages 462-463 of [11].

Because

$$(D.8) \quad \tilde{K}_p(t, \mathbf{x}) = \frac{1}{r^2} \left\{ \text{sinc}(2\pi\omega_0 t) - \frac{1}{2} \begin{bmatrix} \text{sinc}(2\pi\omega_0 [pr - t]) \\ +\text{sinc}(2\pi\omega_0 [pr + t]) \end{bmatrix} \right\}$$

has its Fourier transform

$$(D.9) \quad \int \tilde{K}_p(t, \mathbf{x}) e^{i2\pi(\omega t - \mathbf{k} \cdot \mathbf{x})} dt d\mathbf{x} \\ = 2\pi^2 |\omega p| \chi_{[-1,1]}(\omega \omega_0^{-1}) \operatorname{arcsinh} \left(\frac{\sqrt{(\omega p)^2 - |\mathbf{k}|^2}}{|\mathbf{k}|} \right), \\ 0 < |\mathbf{k}| \leq |\omega p|,$$

supported over

$$(D.10) \quad C_p = \{(\omega, \mathbf{k}) \in \mathbb{R} \times \mathbb{R}^2 \mid \omega \in [-\omega_0, \omega_0], |\mathbf{k}| \leq \omega p\},$$

$\tilde{K}(t, \mathbf{x})$ is C -limited within $\tilde{C} = \{(\omega, \mathbf{k}) \in \mathbb{R} \times \mathbb{R}^2 \mid \omega \in [-\omega_0, \omega_0], |\mathbf{k}| \leq \omega p_{\max} \max_m \{\gamma_m\}\}$. If $\max_m \{\gamma_m\} \approx 1$, then the cone-limit C of $K(t, \mathbf{x})$ is approximated by the cone-limit \tilde{C} of $\tilde{K}(t, \mathbf{x})$ which is the case in practice. For $\omega_0 = 50$ and $p_{\max} = 1$, we present $\tilde{K}(t, \mathbf{x})$ and its Fourier transform in Figure D.1.

For $n = 2$, discretization of the integral representation of $K(t, \mathbf{x})$ can be obtained by

$$(D.11) \quad K(t, \mathbf{x}) = 2p_{\max}^2 \omega_0^3 \int_{-1}^1 \int_0^1 \int_{-1}^1 e^{i2\pi\phi(\omega, p, \tau; t, x, y)} \frac{\omega^2 p}{\sqrt{1 - \tau^2}} d\omega dp d\tau \\ = 2p_{\max}^2 \omega_0^3 \sum_{m, n, l} a_{m, n, l} e^{i2\pi\phi[m, n, l](t, x, y)}$$

where

$$(D.12) \quad a_{m, n, l} = \alpha_m \beta_{m, n} \gamma_{m, n, l} \frac{\omega[m]^2 p[m, n]}{\sqrt{1 - (\tau[m, n, l])^2}}$$

$$(D.13) \quad \phi(\omega, p, \tau; t, x, y) = \omega_0 \omega (t - p_{\max} p [x\tau + y\sqrt{1 - \tau^2}])$$

$$(D.14) \quad \phi[m, n, l](t, x, y) = \omega_0 \omega [m] (t - p_{\max} p [m, n] [x\tau[m, n, l] + y\sqrt{1 - (\tau[m, n, l])^2}])$$

with $(\alpha_m, \omega[m])$ and $(\beta_{m, n}, p[m, n])$ are quadratures for approximating $\operatorname{sinc}(Bx)$ as a sum of cosines (see (B.2)) for B equal to $4\pi\omega_0(T + p_{\max}R)$ and $2\pi\omega_0\omega[m]p_{\max}R$, respectively, and $(\gamma_{m, n, l}, \tau[m, n, l])$ is the quadrature for approximating $J_0(Bx)$ as a sum of cosines for B equal to $\omega_0\omega[m]p_{\max}p[m, n]R$, where $R = \max_{(t, x, y) \in S+S} \sqrt{x^2 + y^2}$, and $T = \max_{(t, x, y) \in S+S} |t|$, for some region of interest $S \subset \mathbb{R} \times \mathbb{R}^2$. While $(\alpha_m, \omega[m])$ and $(\beta_{m, n}, p[m, n])$ are equivalent to Gauss-Legendre quadrature, and computation of $(\gamma_{m, n, l}, \tau[m, n, l])$ requires solving the following moment problem related to the approximation $J_0(x) \approx \sum_{m=1}^M \alpha_m \cos(\gamma_m x)$, which is equivalent to finding the Clenshaw-Curtis quadrature (see Table 1 in Appendix A).

Note that quadrature for B -limited functions, whose Fourier transforms are supported within a ball $B = \{\mathbf{k} \in \mathbb{R}^n \mid |\mathbf{k}| \leq k_{\max}\}$, can be generated in a similar fashion (see Figure D.3).

SCHLUMBERGER, HIGH CROSS, MADINGLEY ROAD, CAMBRIDGE, CB3 0EL, UNITED KINGDOM
(CYARMAN@SLB.COM)

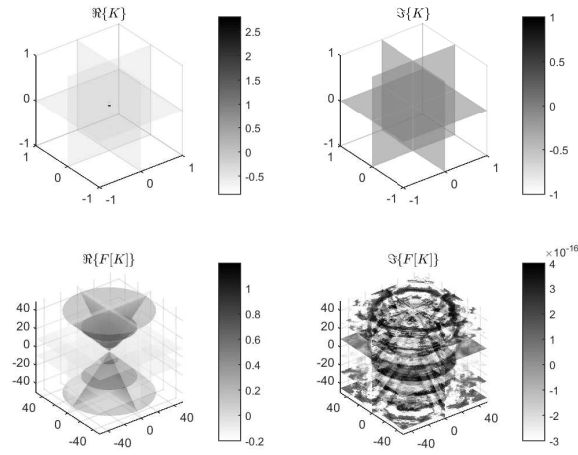


FIGURE D.1. Real, imaginary parts of $\tilde{K}(t, \mathbf{x})$ and its Fourier transform for $\omega_0 = 50$ and $p_{\max} = 1$.

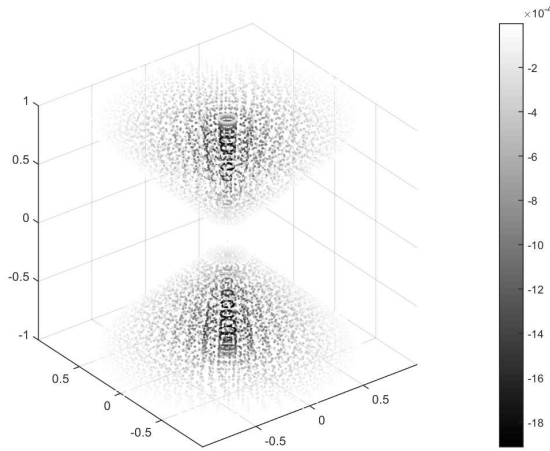


FIGURE D.2. Quadrature $(a_{mnl}, \omega_0(\omega[m], p_{\max} \mathbf{p}[m, n, l]))$ for C -limited functions for $\omega_0 = 1$ and $p_{\max} = 1$.

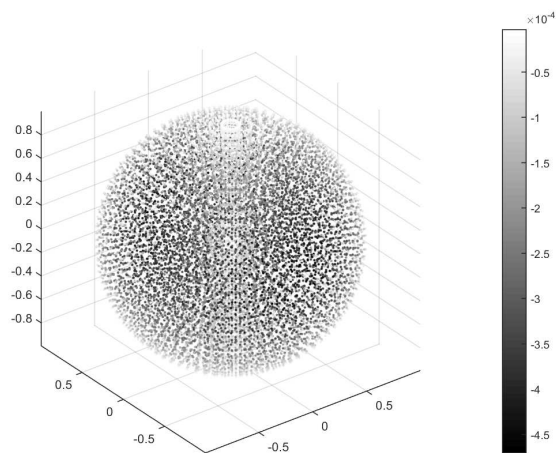


FIGURE D.3. Quadrature $(a_{mnl}, k_{\max} \mathbf{k}_{m,n,l})$ for C -limited functions for $k_{\max} = 1$.